

Chiral Structure and Selection Rules in Light-Front Nucleon-Pentaquark Mixing

Fangcheng He,^{1,2,*} Edward Shuryak,^{3,†} Wan Wu,^{3,4,‡} and Ismail Zahed^{3,§}

¹*Department of Physics, New Mexico State University, Las Cruces, NM 88003, USA*

²*Nuclear Science Division, Lawrence Berkeley National Laboratory, Berkeley, CA 94720, USA*

³*Center for Nuclear Theory, Department of Physics and Astronomy,
Stony Brook University, Stony Brook, New York 11794-3800, USA*

⁴*Physics Department, Tsinghua University, Beijing 100084, China*

We present a light-front Hamiltonian analysis of nucleon–pentaquark mixing induced by σ - and π -type transition operators in a fully Pauli-consistent five-quark basis. The pentaquark configurations are constructed using a systematic permutation-group classification of orbital, spin-flavor, and color degrees of freedom, and the hyperfine interaction is diagonalized to obtain orthonormal eigenchannels with definite quantum numbers. We compute the mixing coefficients for all 27 positive-parity P -wave pentastates and find a highly sparse structure: only 6 channels contribute to the nucleon wave function, while the remaining 21 vanish due to symmetry selection rules. The nonzero contributions are concentrated in a small set of hyperfine eigenchannels, demonstrating a strong dominance pattern. The σ - and π -induced amplitudes populate the same subset of states and are related by a fixed phase, reflecting their common chiral structure, which eliminates interference in the normalization. As a result, their contributions add incoherently, yielding a total five-quark probability of about 29%, with the remaining 71% residing in the three-quark core. These results show that nucleon-pentaquark mixing is governed primarily by symmetry selection rules and chiral structure, and that the five-quark content is dominated by a small number of dynamically selected channels.

I. INTRODUCTION

The internal structure of the nucleon in Quantum Chromodynamics is inherently multi-partonic. While the minimal three-quark picture captures the gross quantum numbers of baryons, it is well established that higher Fock components containing explicit quark-antiquark pairs play an important role in spin, flavor, and momentum distributions, as well as in baryon spectroscopy and transition processes [1, 2]. In a light-front description, these effects are naturally encoded in the presence of higher Fock sectors in the baryon wave function, with the lowest nontrivial extension beyond the three-quark sector given by $qqqq\bar{q}$ configurations.

The importance of five-quark components has been emphasized from several complementary perspectives. Early quark-model studies highlighted the role of $qqqq\bar{q}$ admixtures in explaining spin observables, flavor asymmetries, and baryon mass splittings [3, 4]. In parallel, chiral soliton and large- N_c approaches demonstrated that exotic baryonic configurations and meson-baryon dressing arise naturally once collective and topological degrees of freedom are taken into account [5, 6]. More recently, explicit five-quark Fock components have been explored in both phenomenological and lattice-inspired analyses as a mechanism for understanding sea-quark effects and hidden-flavor baryons [7, 8].

A quantitative treatment of such five-quark components requires two essential ingredients. First, one must

construct a complete and Pauli-allowed basis for the internal quantum numbers of the pentaquark system. This is nontrivial because the four quarks are identical fermions, so their combined orbital, spin-flavor, and color wave function must be antisymmetric under the permutation group S_4 , while the full five-body state must be a color singlet. Second, one must specify the microscopic operators that couple the three-quark nucleon sector to the five-quark sector and evaluate the corresponding transition matrix elements in a controlled dynamical framework.

The purpose of this work is to provide both ingredients in a unified and explicit form, and to quantify the resulting nucleon–pentaquark mixing in a light-front Hamiltonian framework. We construct a complete set of Pauli-consistent pentaquark states using a systematic permutation-group classification of orbital, spin-flavor, and color degrees of freedom based on Young tableaux. These states are organized into symmetry-adapted bases that allow for efficient evaluation of matrix elements and a transparent implementation of the Pauli principle. The present work is in the continuation of the work presented recently in [9], which is aimed at addressing the higher Fock sectors of the nucleon and its tomography [10] (and references therein), based on the wealth of multi-particle states discovered by LHCb [11].

In particular, we address nucleon–pentaquark mixing induced by two physically motivated operators. The first is a σ -type 3P_0 pair-creation operator, which creates a quark-antiquark pair in a color-singlet, flavor-singlet, spin-triplet state with one unit of relative orbital angular momentum [12, 13]. The second is a π -type spin-momentum operator that has additional coupling between longitudinal momentum fractions and spin degrees

* fangchenghe123@gmail.com

† edward.shuryak@stonybrook.edu

‡ wuw20@mails.tsinghua.edu.cn

§ ismail.zahed@stonybrook.edu

of freedom, in close analogy with pion-induced transitions in light-front Hamiltonian approaches [9]. These operators form a chiral pair and impose strong and complementary selection rules on the allowed pentaquark configurations as we will show.

We evaluate the corresponding transition matrix elements in a light-front basis, separating color-spin-flavor recoupling from longitudinal and transverse orbital overlaps. Hyperfine color-spin interactions are included and diagonalized in the pentaquark sector, yielding orthonormal eigenchannels that reorganize the symmetry basis into physically relevant states [14]. The physical nucleon is then constructed as a dressed state containing admixtures of these eigenchannels, with coefficients determined by the transition matrix elements and energy denominators following [9].

A central result of this work is that nucleon-pentaquark mixing exhibits a highly constrained and sparse structure. Among the 27 positive-parity P -wave pentastates, only 6 contribute to the nucleon wave function, while the remaining 21 vanish due to symmetry selection rules. The nonzero contributions are concentrated in a small set of hyperfine eigenchannels, revealing a strong dominance pattern in the five-quark admixture. Furthermore, the σ - and π -induced amplitudes populate the same subset of states and are related by a fixed phase, reflecting their common chiral structure. As a result, their interference vanishes in the normalization, and the two contributions add incoherently. After normalization, the nucleon contains a five-quark component of approximately 29%, dominated by a small number of dynamically selected channels.

The organization of this paper is as follows. In Sec. II we present the permutation-group framework and construct explicit Young-basis states for three- and four-quark systems. In Sec. III we assemble the Pauli-consistent five-quark basis and classify the allowed P -wave pentaquark configurations, we calculate the color-spin hyperfine interaction based on these pentaquark configurations. In Sec. IV we introduce the light-front Hamiltonian and construct the corresponding orbital wave functions. In Sec. V we define the σ - and π -type transition operators and derive the associated selection rules and matrix elements. In Sec. VI we construct the physical nucleon state including five-quark admixtures and analyze the resulting mixing pattern, including the role of chiral structure and interference. Our conclusions are in VII. The appendices provide additional technical details: Appendix A and Appendix B summarize the Young-basis constructions and tensor-product projections, while Appendix C and D detail the light-front eigenbasis and numerical implementation of the P -wave pentaquark states and S -wave three quark states, respectively. In Appendix E we give the explicit orbital, spin-flavor, and color (OSFC) form of the nucleon and pentastates. The derivation of chiral relation between σ - and π -type interactions in the Foldy-Wouthuysen reduction is presented in Appendix F.

II. GROUP DECOMPOSITION

The central dynamical problem addressed in this work is the construction of pentaquark states with well-defined total quantum numbers (J^P, I, S, \dots) while enforcing the Pauli principle for the identical quarks. In constituent or effective descriptions, the dynamics is encoded in Hamiltonian matrix elements evaluated in a basis of color \times spin \times flavor \times orbital states. The bottleneck is not only the diagonalization but the faithful construction of a basis that is complete, non-redundant, and automatically antisymmetric under exchange of identical quarks.

For a $qqqq\bar{q}$ system with four identical quarks, the Pauli constraint is most conveniently implemented at the level of the permutation group S_4 acting on the four-quark labels. One organizes the four-quark wavefunction into irreducible representations (irreps) $[f]$ of S_4 , with the understanding that the total four-quark state must be antisymmetric under any quark exchange. Since the full wavefunction factors into orbital, spin-flavor, and color parts (and sometimes additional internal labels), each factor transforms in some S_4 irrep; the product of these irreps must contain the totally antisymmetric irrep [111]. This section fixes explicit Young-basis states and projection formulas that will be repeatedly invoked when coupling subsystems, counting independent states, and evaluating symmetry-constrained matrix elements.

Two levels of permutation structure appear in practice. For internal couplings that single out a three-quark cluster (e.g. when relating a four-quark core to baryon-like substructures or when defining Jacobi coordinates), S_3 enters naturally. For the full four-quark core, S_4 controls the allowed symmetry patterns. Because the subsequent sections require explicit coefficients (rather than abstract group-theory statements), we provide normalized Young-basis vectors and explicit tensor-product projections. These are the concrete bookkeeping rules behind phrases such as “mixed symmetry” or “Pauli-allowed coupling” and they directly determine which dynamical channels exist.

A. Three-quark Young basis and physical interpretation

For three quarks, the relevant permutation irreps are the fully symmetric [3] and the mixed-symmetry [21]. The totally antisymmetric irrep [111] also exists, but for most spin-flavor applications with three quarks it enters implicitly through color (e.g. a baryon color wavefunction is [111] under S_3), leaving the spin-flavor and orbital factors to be symmetric or mixed such that the total is antisymmetric. The practical lesson is that for any three-quark subcluster the exchange symmetry dictates selection rules: operators symmetric under exchanges couple only to the symmetric components, while exchange-odd structures project onto mixed/antisymmetric components.

To make these statements operational, we adopt an explicit normalized Young basis in a two-state label space $\{i_1, i_2\}$. This two-state space can be viewed as a pedagogical stand-in for any binary internal label (e.g. a reduced flavor doublet, or a spin- $\frac{1}{2}$ projection basis) used to build symmetry-adapted combinations. The algebra of S_3 does not depend on the physical meaning of the label; only the action of permutations matters.

A convenient normalized basis is

$$\begin{aligned} [3] &= |i_1 i_1 i_1\rangle, \\ [21]_\alpha &= \frac{1}{\sqrt{2}}(|i_1 i_2\rangle - |i_2 i_1\rangle) |i_1\rangle, \\ [21]_\beta &= \frac{1}{\sqrt{6}}(2|i_1 i_1 i_2\rangle - |i_1 i_2 i_1\rangle - |i_2 i_1 i_1\rangle). \end{aligned} \quad (1)$$

The two mixed-symmetry vectors correspond to the two standard Young tableaux of [21],

$$[21]_\alpha = \begin{array}{|c|c|} \hline 1 & 3 \\ \hline 2 & \\ \hline \end{array}, \quad [21]_\beta = \begin{array}{|c|c|} \hline 1 & 2 \\ \hline 3 & \\ \hline \end{array}. \quad (2)$$

Physically, the distinction between α and β is a choice of coupling order and basis within the same irrep; the subscript keeps track of which Young operator has been applied. In later matrix elements, this label becomes important because intermediate couplings (e.g. coupling quarks 1, 2 first versus 2, 3 first) lead to different recoupling coefficients.

The normalization conventions above are chosen so that inner products are orthonormal within each irrep, and so that the subsequent tensor-product projection coefficients are simple square roots. These conventions are also convenient when the same S_3 irrep appears in different physical sectors (spin, flavor, orbital), because they allow one to reuse identical projection formulae. More details can be found in Appendix A.

B. Four-quark Young basis and why it matters for pentaquarks

For four identical quarks, the permutation group is S_4 and the relevant irreps are

$$[4], \quad [31], \quad [22], \quad [211], \quad [1111]. \quad (3)$$

In pentaquark construction, [1111] plays the role of the Pauli target: the total four-quark wavefunction must transform as [1111] under S_4 . The four-quark wavefunction factorizes into

$$\Psi_{4q} = \Psi_{\text{orb}} \Psi_{\text{spin-flavor}} \Psi_{\text{color}}, \quad (4)$$

so that the allowed symmetry types are those for which

$$[f_{\text{orb}}] \otimes [f_{\text{spin-flavor}}] \otimes [f_{\text{color}}] \supset [1111]. \quad (5)$$

This single inclusion condition is the group-theoretic statement of the Pauli principle. It enforces, for example, that if the orbital state is symmetric [4] (ground-state S -wave for the four-quark core), then the combined spin \otimes flavor \otimes color must be [1111]. If instead the orbital part is mixed (e.g. a single P -wave excitation corresponds typically to [31]), then spin \otimes flavor \otimes color must compensate accordingly. Thus the decomposition tables below are not ornamental: they specify which orbital excitations can coexist with which color-spin-flavor patterns and therefore which physical channels exist.

As in the S_3 case, we present explicit normalized Young-basis vectors in a two-state label space $\{i_1, i_2\}$. Again this is a concrete representation used to fix phases and normalizations of basis states. In actual applications the labels will correspond to spin projections, isospin components, strange/nonstrange flavor indices, or orbital single-particle labels; the S_4 symmetry algebra is the same.

A normalized basis for the S_4 irreps [4], [31], and [22] is

$$\begin{aligned}
[4] &= |i_1 i_1 i_1 i_1\rangle, \\
[31]_\alpha &= \frac{1}{\sqrt{2}}(|i_1 i_2\rangle - |i_2 i_1\rangle) |i_1 i_1\rangle, \\
[31]_\beta &= \frac{1}{\sqrt{6}}(2|i_1 i_1 i_2\rangle - |i_1 i_2 i_1\rangle - |i_2 i_1 i_1\rangle) |i_1\rangle, \\
[31]_\gamma &= \frac{1}{\sqrt{12}}(3|i_1 i_1 i_1 i_2\rangle - |i_2 i_1 i_1 i_1\rangle - |i_1 i_2 i_1 i_1\rangle - |i_1 i_1 i_2 i_1\rangle), \\
[22]_\alpha &= \sqrt{\frac{1}{4}}(|i_1 i_2 i_1 i_2\rangle - |i_2 i_1 i_1 i_2\rangle - |i_1 i_2 i_2 i_1\rangle + |i_2 i_1 i_2 i_1\rangle), \\
[22]_\beta &= \sqrt{\frac{1}{12}}(2|i_1 i_1 i_2 i_2\rangle - |i_1 i_2 i_1 i_2\rangle - |i_2 i_1 i_1 i_2\rangle - |i_1 i_2 i_2 i_1\rangle - |i_2 i_1 i_2 i_1\rangle + 2|i_2 i_2 i_1 i_1\rangle).
\end{aligned} \tag{6}$$

The three basis vectors of the [31] irrep are labeled by α, β, γ and are defined by the standard Young tableaux; they enter naturally when coupling mixed-symmetry factors to produce an overall antisymmetric four-quark core. The corresponding Young tableaux are

$$[31]_\alpha = \begin{array}{|c|c|c|} \hline 1 & 3 & 4 \\ \hline 2 & & \\ \hline \end{array}, \quad [31]_\beta = \begin{array}{|c|c|c|} \hline 1 & 2 & 4 \\ \hline 3 & & \\ \hline \end{array}, \quad [31]_\gamma = \begin{array}{|c|c|c|} \hline 1 & 2 & 3 \\ \hline 4 & & \\ \hline \end{array}, \tag{7}$$

$$[22]_\alpha = \begin{array}{|c|c|} \hline 1 & 3 \\ \hline 2 & 4 \\ \hline \end{array}, \quad [22]_\beta = \begin{array}{|c|c|} \hline 1 & 2 \\ \hline 3 & 4 \\ \hline \end{array}. \tag{8}$$

The irrep [31] is the archetype of “one unit of mixed symmetry”: individual basis states transform into each other under permutation. In orbital language, this irrep is the typical symmetry of a single P -wave excitation of an otherwise symmetric four-body configuration; in spin-flavor language it corresponds to a core where three quarks are in a mixed symmetric pattern and one quark plays a distinguished role. The irrep [22] is “pairwise” symmetry and is especially common in diquark-like decompositions where (12) and (34) are correlated pairs.

For [211] we label the three standard basis vectors by α, β, γ through their tableaux

$$[211]_\alpha = \begin{array}{|c|c|} \hline 1 & 3 \\ \hline 2 & \\ \hline 4 & \\ \hline \end{array}, \quad [211]_\beta = \begin{array}{|c|c|} \hline 1 & 2 \\ \hline 3 & \\ \hline 4 & \\ \hline \end{array}, \quad [211]_\gamma = \begin{array}{|c|c|} \hline 1 & 4 \\ \hline 2 & \\ \hline 3 & \\ \hline \end{array}. \tag{9}$$

In later sections [211] appears naturally when coupling a mixed-symmetry factor to another mixed-symmetry factor and demanding an overall antisymmetric four-quark core. More details can be found in Appendix B.

C. Explicit tensor-product projections

Once a symmetry-adapted basis is chosen, two tasks recur throughout the pentaquark analysis.

First, one must decide which combinations of orbital, spin-flavor, and color irreps can yield a Pauli-allowed four-quark state. This is a tensor-product question in

S_4 and is solved by decomposition rules such as

$$[31] \otimes [31] = [4] \oplus [31] \oplus [22] \oplus [211]. \tag{10}$$

Second, having identified the allowed irreps, one must actually build normalized states and compute matrix elements. This requires explicit projection coefficients that map products of basis vectors into a definite irrep, because Hamiltonians are typically sums of two-body operators symmetric under particle relabeling, and their reduced matrix elements depend sensitively on these projections.

The formulas below provide exactly these projections. The notation

$$([f]_{AB} : [f_A]_A \otimes [f_B]_B) \tag{11}$$

denotes the normalized projection of a product state transforming in irrep f_A of physical factor A and irrep f_B of physical factor B onto the irrep $[f]$ in the combined AB space. (for example, A might denote spin symmetry, B might denote color symmetry and AB is the spin-color space.)

The explicit Young-basis states and projectors assembled here and in Appendix A-B serve three concrete purposes in the remainder of the manuscript. They provide a systematic enumeration of Pauli-allowed $qqqq$ cores for a given orbital symmetry (most crucially, distinguishing S -wave [4] from P -wave [31] excitations). They fix the relative phases between different coupling schemes, which is essential when assembling total states with the antiquark and when comparing to alternative clusterizations such

as baryon-meson versus diquark-triquark. They allow us to evaluate matrix elements of permutation-symmetric two-body operators by reducing them to reduced matrix elements within definite S_4 irreps, thereby separating dynamics from symmetry.

In the next section we will use these projections to construct explicit pentaquark basis states with definite color singlet structure, and to tabulate the resulting (S, I) multiplets and their parity assignments for both S -wave and P -wave cores.

III. FIVE-QUARK DECOMPOSITION

This section assembles the explicit $|qqqq\bar{q}\rangle$ basis used throughout the dynamical analysis of nucleon-pentaquark mixing on the light front. The goal is not to re-derive the permutation-group machinery already fixed in Sec. II, but to show how that machinery becomes a practical “interface” between (i) Pauli consistency for the q^4 core, (ii) hyperfine diagonalization in the positive-parity P -wave sector, and (iii) the transition operators that connect $|qqq\rangle$ and $|qqqq\bar{q}\rangle$ Fock sectors.

We build the pentaquark state from a four-quark core (q^4) coupled to an antiquark \bar{q} . The four quarks are identical fermions, so the complete four-quark wave function must be antisymmetric under S_4 permutations: the product of orbital (L), spin-flavor (SF), and color (C) symmetry types must contain the fully antisymmetric irrep [1111]. The explicit Young-basis conventions and all required S_4 tensor-product projections are fixed once and for all in this section; we use them here without repetition.

For the positive-parity pentaquarks of interest, the orbital part carries one unit of relative angular momentum. In the four-quark sector this implies orbital permutation symmetry $L[4]$ or $L[31]$, depending on which Jacobi coordinate carries the P -wave excitation. Color is chosen as $C[211]$ for the q^4 core so that coupling to the antiquark color $\mathbf{3}$ yields an overall color singlet. With these ingredients, the remaining task is to enumerate and write the canonical OSFC basis states in a form that makes both hyperfine matrix elements and transition operators straightforward to evaluate.

A. Pauli-consistent OSFC bookkeeping for the q^4 core

The key reason to work in an S_4 -irrep basis is that the operators that drive both spectroscopy and mixing are built from pairwise structures acting inside the q^4 core. Hyperfine interactions are sums of two-body color-spin operators (schematically $\lambda_i \cdot \lambda_j \sigma_i \cdot \sigma_j$), while the transition operators that connect $|qqq\rangle$ to $|qqqq\bar{q}\rangle$ select very specific spin and orbital components of the five-quark wave function. In an S_4 -adapted basis, permutations P_{ij} act as sparse linear maps organized by $[f]$ labels, so the sym-

metry reduction is performed once (through the Sec. III projectors) and then reused uniformly in every matrix element.

Concretely, we label a four-quark configuration by its orbital symmetry $[f]_L$, spin-flavor symmetry $[f']_{SF}$, and color symmetry $C[211]$, and we couple these sectors so that the resulting q^4 state is Pauli allowed. The corresponding five-quark state is obtained by coupling the antiquark color to make a singlet, and the antiquark spin-flavor quantum numbers are appended in the usual way. This construction keeps the orbital dependence explicit through P -wave functions φ_{m_L} or $\tilde{\varphi}_{1m_L}$ carrying the magnetic projection m_L , while the internal OSFC structure is handled algebraically by the S_4 projectors.

B. Counting of P -wave pentaquarks

The allowed P -wave configurations are determined by which $(L \otimes SF)$ symmetry types can combine with color $C[211]$ to produce an antisymmetric four-quark core. For the present construction we focus on total isospin $I = \frac{1}{2}$ and spins $S = \frac{1}{2}, \frac{3}{2}, \frac{5}{2}$. A compact bookkeeping is to list the admissible $(L[f] \otimes SF[f'])$ families and count the multiplicities in each (I, S) channel.

The resulting number of P -wave states is summarized in Table I.

<i>num</i>	$I = \frac{1}{2} \ S = \frac{1}{2}$	$I = \frac{1}{2} \ S = \frac{3}{2}$	$I = \frac{1}{2} \ S = \frac{5}{2}$
$L[4] \otimes SF[31]$	3	3	1
$L[31] \otimes SF[31]$	3	3	1
$L[31] \otimes SF[22]$	2	2	1
$L[31] \otimes SF[4]$	2	1	0
$L[31] \otimes SF[211]$	3	2	0
<i>Total</i>	13	11	3

TABLE I: The number of P -wave states in the pentaquark basis for $I = \frac{1}{2}$ and the listed spins S .

It is also useful to indicate representative decompositions of five-quark spin-flavor configurations into separate flavor and spin irreps. For the channels emphasized here, the dominant decompositions are listed in Table II.

$I = \frac{1}{2} \ S = \frac{1}{2}$	$I = \frac{1}{2} \ S = \frac{3}{2}$	$I = \frac{1}{2} \ S = \frac{5}{2}$
$F[22] \ S[22]$	$F[22] \ S[31]$	$F[22] \ S[4]$
$F[31] \ S[31]$	$F[31] \ S[4]$	$F[31] \ S[4]$

TABLE II: Representative decompositions of five-quark spin-flavor configurations into separate flavor and spin irreps.

C. Canonical P -wave pentaquark wave functions

We now write the canonical P -wave pentaquark states in the OSFC basis, with a four-quark color core in $C[211]$

coupled to the antiquark to form an overall color singlet. The internal OSFC structure is fixed by the requirement that the four-quark core be antisymmetric under S_4 once orbital, spin-flavor, and color are combined.

We first define the $L[4] \otimes SF[31]$ family:

$$\Psi_{Pm_L}^A = \frac{1}{\sqrt{3}} \left(\left[C[211]_\beta (L[4]SF[31])_\alpha - C[211]_\alpha (L[4]SF[31])_\beta + C[211]_\gamma (L[4]SF[31])_\gamma \right] C[11] SF[1] \right). \quad (12)$$

The spin-flavor substructures needed in later projections can be organized as

$$\begin{aligned} & L[4] (SF[31] : F[31] \otimes S[31])_{\alpha,\beta,\gamma}, \\ & L[4] (SF[31] : F[22] \otimes S[31])_{\alpha,\beta,\gamma}, \\ & L[4] (SF[31] : F[31] \otimes S[22])_{\alpha,\beta,\gamma}, \\ & L[4] (SF[31] : F[31] \otimes S[4])_{\alpha,\beta,\gamma}, \end{aligned} \quad (13)$$

The last one is for $S = 5/2$ and $S = 3/2$ cases. Next, for the $L[31] \otimes SF[4]$ family we define

$$\Psi_P^P = \frac{1}{\sqrt{3}} \left(\left[C[211]_\beta (L[31]SF[4])_\alpha - C[211]_\alpha (L[31]SF[4])_\beta + C[211]_\gamma (L[31]SF[4])_\gamma \right] C[11] SF[1] \right), \quad (14)$$

with the corresponding SF couplings

$$\begin{aligned} & (L[31] (SF[4] : F[31]S[31]))_{\alpha,\beta,\gamma}, \\ & (L[31] (SF[4] : F[22]S[22]))_{\alpha,\beta,\gamma}. \end{aligned} \quad (15)$$

For the $L[31] \otimes SF[31]$ family we define

$$\Psi_{P1}^P = \frac{1}{\sqrt{3}} \left(\left[C[211]_\beta (L[31]SF[31])_\alpha - C[211]_\alpha (L[31]SF[31])_\beta + C[211]_\gamma (L[31]SF[31])_\gamma \right] C[11] SF[1] \right), \quad (16)$$

with

$$\begin{aligned} & (L[31] (SF[31] : F[31]S[31]))_{\alpha,\beta,\gamma}, \\ & (L[31] (SF[31] : F[22]S[31]))_{\alpha,\beta,\gamma}, \\ & (L[31] (SF[31] : F[31]S[22]))_{\alpha,\beta,\gamma}, \\ & (L[31] (SF[31] : F[31]S[4]))_{\alpha,\beta,\gamma}. \end{aligned} \quad (17)$$

Finally, the remaining $L[31] \otimes SF[22]$ and $L[31] \otimes SF[211]$ families are

$$\Psi_{P2}^P = \frac{1}{\sqrt{3}} \left(\left[C[211]_\beta (L[31]SF[22])_\alpha - C[211]_\alpha (L[31]SF[22])_\beta + C[211]_\gamma (L[31]SF[22])_\gamma \right] C[11] SF[1] \right), \quad (18)$$

$$\Psi_{P3}^P = \frac{1}{\sqrt{3}} \left(\left[C[211]_\beta (L[31]SF[211])_\alpha - C[211]_\alpha (L[31]SF[211])_\beta + C[211]_\gamma (L[31]SF[211])_\gamma \right] C[11] SF[1] \right). \quad (19)$$

with

$$\begin{aligned} & (L[31] (SF[22] : F[31]S[31]))_{\alpha,\beta,\gamma}, \\ & (L[31] (SF[22] : F[22]S[22]))_{\alpha,\beta,\gamma}, \\ & (L[31] (SF[22] : F[22]S[4]))_{\alpha,\beta,\gamma}, \end{aligned} \quad (20)$$

and

$$\begin{aligned} & (L[31] (SF[211] : F[31]S[31]))_{\alpha,\beta,\gamma}, \\ & (L[31] (SF[211] : F[22]S[31]))_{\alpha,\beta,\gamma}, \\ & (L[31] (SF[211] : F[31]S[22]))_{\alpha,\beta,\gamma}, \end{aligned} \quad (21)$$

In summary, the 13 states with $(I = \frac{1}{2}, S = \frac{1}{2})$ can be labeled as

$$\begin{aligned}
LSF = & L[4]SF[31]_a : S[31] \otimes F[31], & L[4]SF[31]_b : S[31] \otimes F[22], & L[4]SF[31]_c : S[22] \otimes F[31] \\
& L[31]SF[31]_a : S[31] \otimes F[31], & L[31]SF[31]_b : S[31] \otimes F[22], & L[31]SF[31]_c : S[22] \otimes F[31] \\
& L[31]SF[22]_a : S[31] \otimes F[31], & L[31]SF[22]_b : S[22] \otimes F[22], & \\
& L[31]SF[4]_a : S[31] \otimes F[31], & L[31]SF[4]_b : S[22] \otimes F[22], & \\
& L[31]SF[211]_a : S[31] \otimes F[31], & L[31]SF[211]_b : S[31] \otimes F[22], & L[31]SF[211]_c : S[22] \otimes F[31](22)
\end{aligned}$$

The 11 states with $(I = \frac{1}{2}, S = \frac{3}{2})$ can be labeled as

$$\begin{aligned}
LSF = & L[4]SF[31]_a : S[31] \otimes F[31], & L[4]SF[31]_b : S[31] \otimes F[22], & L[4]SF[31]_c : S[4] \otimes F[31] \\
& L[31]SF[31]_a : S[31] \otimes F[31], & L[31]SF[31]_b : S[31] \otimes F[22], & L[31]SF[31]_c : S[4] \otimes F[31] \\
& L[31]SF[22]_a : S[31] \otimes F[31], & L[31]SF[22]_b : S[4] \otimes F[22], & \\
& L[31]SF[4] : S[31] \otimes F[31], & & \\
& L[31]SF[211]_a : S[31] \otimes F[31], & L[31]SF[211]_b : S[31] \otimes F[22] & (23)
\end{aligned}$$

The three states with $(I = \frac{1}{2}, S = \frac{5}{2})$ can be labeled as

$$\begin{aligned}
LSF = & L[4]SF[31] : S[4] \otimes F[31] \\
& L[31]SF[31] : S[4] \otimes F[31] \\
& L[31]SF[22] : S[4] \otimes F[22], & (24)
\end{aligned}$$

The labels $L[4]$ and $L[31]$ represent the light-cone P wave state, they are the functions of longitudinal momentum x_ξ and transverse momentum $k_{\xi,\perp}$ in Jacobi coordinates, we will show later how to construct them using the eigenstates of light cone Hamiltonian. The full pentaquark wavefunction can be found in Appendix E 2.

D. Color-spin hyperfine interaction including antiquark effects

The short-range dynamics of the pentaquark is governed by the color-spin hyperfine interaction induced by

$$H_{CS} = - \sum_{i < j \leq 5} \frac{V_{1g}(r_{ij})}{m_Q^2} \lambda_{ij} \Sigma_{ij} = - \frac{V_{1g}(r_{ij})}{m_Q^2} \left(\sum_{i < j}^4 \lambda_i \cdot \lambda_j \sigma_i \cdot \sigma_j + \sum_{i=1}^4 \lambda_i \cdot \lambda_{\bar{q}} \sigma_i \cdot \sigma_{\bar{q}} \right), \quad (25)$$

where λ_i and σ_i act on the color and spin of quark i , while $\lambda_{\bar{q}} = -\lambda^*$ and $\sigma_{\bar{q}} = -\sigma^*$ act on the antiquark.

Assuming the Δ -nucleon mass splitting to be saturated by the color-spin interaction, we have

$$M_\Delta - M_N = \frac{16V_{1g}}{m_Q^2} \rightarrow (1232 - 939) \text{ MeV}. \quad (26)$$

The first term in Eq. (25) acts entirely within the q^4 subsystem. Since it is fully symmetric under permutations of the four quarks, its matrix elements are block diagonal in irreducible representations of the permutation

one-gluon exchange. For a genuine five-body system this interaction acts not only among the four identical quarks but also between each quark and the antiquark. The full hyperfine Hamiltonian therefore takes the form

group S_4 . This implies that it does not mix states belonging to different S_4 irreps, although off-diagonal matrix elements may appear between different basis vectors within the same irrep.

The second term involves the antiquark and couples each quark individually to the antiquark. Although the total color operator satisfies

$$\sum_{i=1}^4 \lambda_i \cdot \lambda_{\bar{q}} = -\frac{16}{3} \quad (27)$$

in a color-singlet $q^4\bar{q}$ state, the operator

$$\sum_{i=1}^4 (\boldsymbol{\lambda}_i \cdot \boldsymbol{\lambda}_{\bar{q}}) (\boldsymbol{\sigma}_i \cdot \boldsymbol{\sigma}_{\bar{q}}) \quad (28)$$

does not in general factorize into a universal color coefficient times a spin factor depending only on total spins. Its matrix elements depend on the full color-spin recoupling structure of the basis states.

We evaluate the hyperfine interaction in the OSFC basis, in which the four-quark subsystem is first coupled to definite color $C[211]$, spin S_{q^4} , and spin-flavor symmetry, and then combined with the antiquark to form a total color singlet and total spin S . The four-quark core spin takes integer values

$$S_{q^4} = 0, 1, 2, \quad (29)$$

which couple with the antiquark spin 1/2 to give total pentaquark spin

$$S = \frac{1}{2}, \frac{3}{2}, \frac{5}{2}. \quad (30)$$

In this basis, both the quark-quark and quark-antiquark parts of the hyperfine interaction are evaluated directly using standard color and spin recoupling. For the quark-quark term,

$$H_{qq} = -\frac{V_{1q}(r_{ij})}{m_Q^2} \sum_{i<j}^4 (\boldsymbol{\lambda}_i \cdot \boldsymbol{\lambda}_j) (\boldsymbol{\sigma}_i \cdot \boldsymbol{\sigma}_j), \quad (31)$$

the operator is invariant under permutations of the four quarks and therefore preserves the S_4 symmetry of the OSFC basis. Off-diagonal matrix elements arise from recoupling between different Young basis vectors within the same symmetry sector.

For the quark-antiquark term,

$$H_{q\bar{q}} = -\frac{V_{1q}(r_{ij})}{m_Q^2} \sum_{i=1}^4 (\boldsymbol{\lambda}_i \cdot \boldsymbol{\lambda}_{\bar{q}}) (\boldsymbol{\sigma}_i \cdot \boldsymbol{\sigma}_{\bar{q}}), \quad (32)$$

each quark contributes separately, and the resulting matrix elements depend on the detailed color-spin structure of the OSFC basis states. In the present basis, this operator is diagonal or block diagonal, but its diagonal values are state-dependent and cannot be expressed solely in terms of (S_{q^4}, S) .

The full hyperfine matrices are therefore constructed directly in the OSFC basis for each (I, S) sector. The explicit matrices for isospin $I = \frac{1}{2}$ and total spins $S = \frac{1}{2}, \frac{3}{2}, \frac{5}{2}$ are given in Tables III, IV and V below. These matrices include both diagonal contributions and off-diagonal mixings arising from quark-quark recoupling.

Diagonalization of these matrices yields orthonormal hyperfine eigenchannels, which provide the physical pentaquark basis used in the subsequent nucleon dressing and mixing analysis.

E. Connection to Young tableaux

The computation of the explicit color-spin matrices is most transparent when formulated in the Young-tableaux language used throughout the OSFC construction. The central point is that the four identical quarks furnish a representation of the permutation group S_4 , and the Pauli principle requires the q^4 wavefunction to be antisymmetric, i.e. to transform as $[1111]$ under S_4 . In the OSFC basis each factor—orbital, spin-flavor, and color—is assigned an S_4 Young pattern, and the allowed pentaquark basis vectors are those for which the tensor product

$$[f]_L \otimes [f]_{\text{SF}} \otimes [f]_C \supset [1111] \quad (33)$$

contains the fully antisymmetric irrep. With color fixed to $[211]_C$ in the q^4 sector so that $[211]_C \otimes \bar{\mathbf{3}}_C \rightarrow \mathbf{1}_C$, the orbital patterns relevant for positive-parity P -wave pentaquarks are $L[4]$ and $L[31]$, and the spin-flavor Young patterns $[f]_{\text{SF}}$ are constrained accordingly.

Once the OSFC basis is fixed, the hyperfine operator is evaluated using explicit Young basis vectors. For the quark-quark part (31), one exploits the fact that the operator is invariant under S_4 permutations of the quark labels. Therefore it can only connect states within the same S_4 irrep and is block diagonal in the S_4 -adapted OSFC basis. The actual matrix elements are obtained by evaluating the two-body operator in a basis where a chosen pair, is first coupled in color and spin, and then recoupled back to the chosen OSFC-Young basis.

Concretely, the color factor for a quark pair depends only on whether the pair is in the $\bar{\mathbf{3}}_C$ or $\mathbf{6}_C$ channel,

$$\boldsymbol{\lambda}_i \cdot \boldsymbol{\lambda}_j = \begin{cases} -\frac{8}{3}, & (qq)_{\bar{\mathbf{3}}_C}, \\ +\frac{4}{3}, & (qq)_{\mathbf{6}_C}, \end{cases} \quad (34)$$

while the spin factor depends only on whether the pair is in $s_{ij} = 0$ or $s_{ij} = 1$,

$$\boldsymbol{\sigma}_i \cdot \boldsymbol{\sigma}_j = \begin{cases} -3, & s_{ij} = 0, \\ +1, & s_{ij} = 1. \end{cases} \quad (35)$$

Thus, for any OSFC state $|\Psi_\alpha\rangle$, the contribution of a given pair (ij) is fixed once the amplitudes for finding that pair in the allowed color-spin channels are known. These amplitudes are determined by the Young-tableaux recoupling coefficients (isoscalar factors) relating the pair-coupled basis to the chosen OSFC basis. Summing over all six pairs yields the diagonal entries and, in sectors where multiple Young basis vectors exist with the same quantum numbers, the off-diagonal mixings that appear in the explicit matrices.

The quark-antiquark term in (32) is evaluated in the same OSFC basis. Although the total color contraction is fixed in a color-singlet $q^4\bar{q}$ state,

$$\left(\sum_{i=1}^4 \boldsymbol{\lambda}_i + \boldsymbol{\lambda}_{\bar{q}} \right) |\mathbf{1}_C\rangle = 0, \quad (36)$$

	[4][31] _a	[4][31] _b	[4][31] _c	[31][31] _a	[31][31] _b	[31][31] _c	[31][22] _a	[31][22] _b	[31][4] _a	[31][4] _b	[31][211] _a	[31][211] _b	[31][211] _c
[4][31] _a	$-\frac{16}{3}$		8										
[4][31] _b		$\frac{56}{3}$											
[4][31] _c	8		0										
[31][31] _a				$-\frac{4}{3}$		4	$-8\sqrt{\frac{2}{3}}$		$-\frac{32}{\sqrt{3}}$		-12		$4\sqrt{3}$
[31][31] _b					$\frac{56}{3}$			$4\sqrt{2}$		$-8\sqrt{2}$		$-8\sqrt{3}$	
[31][31] _c				4		12	$8\sqrt{\frac{2}{3}}$		$-\frac{16}{\sqrt{3}}$		-4		$4\sqrt{3}$
[31][22] _a				$-8\sqrt{\frac{2}{3}}$		$8\sqrt{\frac{2}{3}}$	$\frac{16}{3}$		$-\frac{8\sqrt{2}}{3}$		$-8\sqrt{6}$		
[31][22] _b					$4\sqrt{2}$			8		-8		$-4\sqrt{6}$	
[31][4] _a				$-\frac{32}{\sqrt{3}}$		$-\frac{16}{\sqrt{3}}$	$-\frac{8\sqrt{2}}{3}$		8				
[31][4] _b					$-8\sqrt{2}$			-8		8			
[31][211] _a				-12		-4	$-8\sqrt{6}$				$-\frac{4}{3}$		$-4\sqrt{3}$
[31][211] _b					$-8\sqrt{3}$			$-4\sqrt{6}$				$\frac{8}{3}$	
[31][211] _c				$4\sqrt{3}$		$4\sqrt{3}$					$-4\sqrt{3}$		4

TABLE III: Color-spin hyperfine matrix $\sum_{i<j\leq 5} \lambda_{ij} \Sigma_{ij}$ for $I = \frac{1}{2}$ and $S = \frac{1}{2}$. The first number in the bracket denotes the representation for the orbital part, while the second corresponds to the spin-flavor representation. For example, [4][31]_a represents the state $L[4]SF[31]_a$.

	[4][31] _a	[4][31] _b	[4][31] _c	[31][31] _a	[31][31] _b	[31][31] _c	[31][22] _a	[31][22] _b	[31][4]	[31][211] _a	[31][211] _b
[4][31] _a	$-\frac{4}{3}$		$4\sqrt{10}$								
[4][31] _b		$-\frac{4}{3}$									
[4][31] _c	$4\sqrt{10}$		0								
[31][31] _a				$-\frac{10}{3}$		$2\sqrt{10}$	$-2\sqrt{\frac{2}{3}}$		$-\frac{8}{\sqrt{3}}$	-6	
[31][31] _b					$\frac{14}{3}$			$-2\sqrt{10}$			$-2\sqrt{3}$
[31][31] _c				$2\sqrt{10}$			$-4\sqrt{\frac{5}{3}}$		$4\sqrt{\frac{10}{3}}$	$-2\sqrt{10}$	
[31][22] _a				$-2\sqrt{\frac{2}{3}}$		$-4\sqrt{\frac{5}{3}}$	$-\frac{8}{3}$		$-\frac{8\sqrt{2}}{3}$	$-2\sqrt{6}$	
[31][22] _b					$-2\sqrt{10}$						$-2\sqrt{30}$
[31][4]				$-\frac{8}{\sqrt{3}}$		$4\sqrt{\frac{10}{3}}$	$-\frac{8\sqrt{2}}{3}$				
[31][211] _a				-6		$-2\sqrt{10}$	$-2\sqrt{6}$			$-\frac{10}{3}$	
[31][211] _b					$-2\sqrt{3}$			$-2\sqrt{30}$			$\frac{2}{3}$

TABLE IV: Color-spin hyperfine matrix for $I = \frac{1}{2}$ and $S = \frac{3}{2}$

the operator itself acts on each quark separately, and its matrix elements depend on the detailed color-spin structure of the basis states.

The spin dependence may be expressed through angular-momentum algebra as

$$\sum_{i=1}^4 \boldsymbol{\sigma}_i \cdot \boldsymbol{\sigma}_{\bar{q}} = 2 \left[S(S+1) - S_{q^4}(S_{q^4}+1) - \frac{3}{4} \right], \quad (37)$$

but this relation alone does not determine the full matrix elements, since the color-spin operator involves correlated pairwise contractions. As a result, the quark-antiquark contribution is diagonal or block diagonal in the OSFC basis but is generally state-dependent.

To illustrate how an explicit table entry is obtained, one evaluates the matrix element of each pair operator $\boldsymbol{\lambda}_i \cdot \boldsymbol{\lambda}_j \boldsymbol{\sigma}_i \cdot \boldsymbol{\sigma}_j$ by decomposing the state into pair-coupled channels, multiplying by the corresponding eigenvalues, and summing over all six pairs. The quark-antiquark

term is treated analogously, with each quark contributing separately.

IV. THE CONSTRUCTION OF LIGHT-FRONT P-WAVE

The light front Hamiltonian for the pentaquark state includes the kinetic and confining terms

$$H'_{LF} = \sum_{i=1}^5 \left(\frac{k_{i\perp}^2 + m_Q^2}{x_i} + 2\sigma_T((i\partial/\partial x_i)^2 + M^2 r_{i\perp}^2)^{1/2} \right) \quad (38)$$

Here x_i are momentum fractions for quarks, $i = 1..5$ and $r_{i\perp}$ are transverse coordinates. The the string tension $\sigma_T = m_\rho^2/\pi \rightarrow (0.44 \text{ GeV})^2$ is fixed from meson Reggion trajectories, and the mass is approximated as $M \approx 5m_Q$,

	[4][31]	[31][31]	[31][22]
[4][31]	$-\frac{40}{3}$		
[31][31]		$-\frac{40}{3}$	
[31][22]			$-\frac{40}{3}$

TABLE V: Color-spin hyperfine matrix for $I = \frac{1}{2}$ and $S = \frac{5}{2}$

with m_Q the constituent quark mass, which is taken to be 383MeV [15].

To eliminate the motion of center mass, we use the following Jacobi coordinates for the longitudinal part,

$$\begin{aligned}
x_\alpha &= \frac{x_1 - x_2}{\sqrt{2}}, \\
x_\beta &= \frac{x_1 + x_2 - 2x_3}{\sqrt{6}}, \\
x_\gamma &= \frac{x_1 + x_2 + x_3 - 3x_4}{\sqrt{12}}, \\
x_\delta &= \frac{x_1 + x_2 + x_3 + x_4 - 4x_5}{\sqrt{20}} \quad (39)
\end{aligned}$$

Similarly for the transverse part. The light front Hamiltonian, free of CM, can be expressed using Jacobi coordinates [16]

$$\begin{aligned}
H_{LF} &\equiv \sum_{i=1}^5 \frac{k_{i\perp}^2 + m_Q^2}{x_i} + 5\sigma_T a \\
&- \frac{\sigma_T}{a} \sum_{\xi=\alpha,\beta,\gamma,\delta} ((\partial/\partial x_\xi)^2 + M^2(\partial/\partial \vec{k}_{\xi\perp})^2) \quad (40)
\end{aligned}$$

The parameter a is chosen to be $a = 7.59$, which has been determined by minimizing the ground state mass [16]. For the penta quark state, P wave state can be obtained by diagonalizing the full Hamiltonian for five quark states. The longitudinal and transverse eigenbasis used to diagonalize the full Hamiltonian are described in Appendix .C. The P stats for different orbital representation satisfy the following orthogonality conditions

$$\begin{aligned}
\int [d^2\vec{k}_{\perp,\xi}][dx_\xi]\psi_{L[4]}^{\mp 1}(x, k_\perp)e^{\pm i\phi_\delta} &= C_{L[4]}^\perp \delta_{m,\mp 1}, \\
\int [d^2\vec{k}_{\perp,\xi}][dx_\xi]\psi_{L[4]}^0(x, k_\perp)x_j &= C_{L[4]}^\parallel \delta_{j,\delta}, \\
\int [d^2\vec{k}_{\perp,\xi}][dx_\xi]\psi_{L[31]i}^0(x, k_\perp)x_j &= C_{L[31]}^\parallel \delta_{ij} \quad (41)
\end{aligned}$$

where $dx_\xi = dx_\alpha dx_\beta dx_\gamma dx_\delta$ and similarly for $d^2\vec{k}_{\xi\perp}$. $\psi_{L[4]}^n(x, k_\perp)$ and $\psi_{L[31]}^n(x, k_\perp)$ represent light-cone P-wave states for different group representation. Orthogonality conditions are imposed for P-wave states with transverse direction and longitudinal direction, respectively. The coefficients $C_{L[4]}^\perp$, $C_{L[4]}^\parallel$ and $C_{L[31]}^\parallel$ can be obtained once the corresponding P-state states are constructed using the orthogonality conditions described

above. To construct P-wave state, we first calculate the following projections:

$$\begin{aligned}
C_{L[4]}^{n,\pm 1} &= \int [d^2\vec{k}_{\perp,\xi}][dx_\xi]\psi_n(x, k_\perp)e^{\pm i\phi_\delta} \\
C_{L[31]\alpha}^{n,0} &= \int [d^2\vec{k}_{\perp,\xi}][dx_\xi]\psi_n(x, k_\perp)x_\alpha \\
C_{L[31]\beta}^{n,0} &= \int [d^2\vec{k}_{\perp,\xi}][dx_\xi]\psi_n(x, k_\perp)x_\beta \\
C_{L[31]\gamma}^{n,0} &= \int [d^2\vec{k}_{\perp,\xi}][dx_\xi]\psi_n(x, k_\perp)x_\gamma \\
C_{L[31]\delta}^{n,0} &= \int [d^2\vec{k}_{\perp,\xi}][dx_\xi]\psi_n(x, k_\perp)x_\delta \quad (42)
\end{aligned}$$

Here, $\psi_n(x, k_\perp)$ are the eigenstates of the full five quark Hamiltonian. We consider the lowest 11 states, their corresponding energy and projections onto different P-wave components are listed in Table. VI. Using the results in Table. VI, together with orthogonality conditions in Eq. (41), we obtain

$$\begin{aligned}
\psi_{L[4]}^{+1}(x, k_\perp) &= (0.394653 + 0.29994i)\psi_2(x, k_\perp) \\
&+ (-0.24334 + 0.931223i)\psi_3(x, k_\perp) \\
\psi_{L[4]}^{-1}(x, k_\perp) &= (0.641508 - 0.618858i)\psi_2(x, k_\perp) \\
&- (0.334356 + 0.045252i)\psi_3(x, k_\perp) \quad (43)
\end{aligned}$$

One can then calculate the coefficient $C_{L[4]}^\perp$, defined in Eq. (41), as

$$C_{L[4]}^\perp = \int [d^2\vec{k}_{\perp,\xi}][dx_\xi]\psi_{L[4]}^{-1}(x, k_\perp)e^{i\phi_\delta} = 0.469, (44)$$

The state corresponding to the representation $L[31]_\alpha$ is contributed solely by a single eigenstate,

$$\psi_{L[31]\alpha}^0(x, k_\perp) = \psi_8(x, k_\perp) \quad (45)$$

Accordingly, the coefficient $C_{L[31]}^\parallel$ can be obtained as

$$\begin{aligned}
C_{L[31]}^\parallel &= \int [d^2\vec{k}_{\perp,\xi}][dx_\xi]\psi_{L[31]\alpha}^0(x, k_\perp)x_\alpha \\
&= -0.0137 + 0.0465i \quad (46)
\end{aligned}$$

On the other hand, one can verify the following relations

$$\begin{aligned}
|C_{L[31]\alpha}^{8,0}|^2 &\approx |C_{L[31]\beta}^{6,0}|^2 + |C_{L[31]\beta}^{9,0}|^2 \\
&\approx |C_{L[31]\gamma}^{5,0}|^2 + |C_{L[31]\gamma}^{10,0}|^2 \approx |C_{L[4]\delta}^{4,0}|^2 + |C_{L[4]\delta}^{11,0}|^2 \quad (47)
\end{aligned}$$

Therefore, the state corresponding to the representation $L[31]_\beta$ can be expressed as

$$\psi_{L[31]\beta}^0(x, k_\perp) = a_1\psi_6(x, k_\perp) + a_2\psi_9(x, k_\perp) \quad (48)$$

n	$E_n(\text{GeV})$	$C_{L[4]}^{n,+1}$	$C_{L[4]}^{n,-1}$	$C_{L[31]_\alpha}^{n,0}$	$C_{L[31]_\beta}^{n,0}$	$C_{L[31]_\gamma}^{n,0}$	$C_{L[4]_\delta}^{n,0}$
1	4.71	0	0	0	0	0	0
2	4.86	$0.305 + 0.321i$	$0.0988 - 0.1196i$	0	0	0	0
3	4.86	$-0.213 + 0.0813i$	$-0.0859 - 0.4007i$	0	0	0	0
4	4.99	0	0	0	0	0	$0.023 - 0.019i$
5	5.00	0	0	0	0	$-0.023 + 0.017i$	0
6	5.00	0	0	0	$-0.005 + 0.025i$	0	0
7	5.00	0	0	0	0	0	0
8	5.00	0	0	$-0.0137 + 0.0465i$	0	0	0
9	5.05	0	0	0	$0.037 - 0.018i$	0	0
10	5.05	0	0	0	0.0	$-0.038 + 0.003i$	0
11	5.06	0	0	0	0.0	0	$0.003 + 0.037i$

TABLE VI: The projection of lowest 11 states of 5 quark full Hamiltonian. The second column is the energy. The third to eighth columns represent the projections defined in Eq. (42). The ground state shows zero overlap with these P wave projections.

The generic mixing matrix element of interest is of the form

$$\mathcal{M}_{N \leftrightarrow P} = \langle N | \mathcal{O}_{45} | P \rangle, \quad (53)$$

where \mathcal{O}_{45} acts on the created quark-antiquark pair labeled (4, 5) and includes the appropriate color, flavor and spin projectors

$$\chi_{45}^C, \quad \chi_{45}^F, \quad \chi_{45}^S, \quad (54)$$

with χ_{45}^C projecting onto a color singlet, χ_{45}^F onto a flavor singlet, and χ_{45}^S onto the spin channel dictated by the

chosen vertex (triplet for σ -type 3P_0 , and also triplet for the π -type operator used below).

The pentaquark orbital-spin-flavor basis states are labeled as in the tables, e.g. $L[4] SF[31]_{a,b,c}$, $L[31] SF[31]_{a,b,c}$, $L[31] SF[22]_{a,b}$, etc., with the explicit spin-flavor factorization $SF = S[\cdot] \otimes F[\cdot]$ indicated in the captions.

B. σ -type and π -type mixing operators (3P_0 model) and selection rules

The σ -type and π -type mixings are induced by a 3P_0 pair-creation vertex. In momentum space, a standard form is

$$T_{\sigma,\pi} = -3\gamma_0 \int d\vec{p}_4 d\vec{p}_5 \delta(\vec{p}_4 + \vec{p}_5) e^{-r_\sigma^2(\vec{p}_4 - \vec{p}_5)^2/6} \mathcal{T}_{\sigma,\pi} \chi_{45}^F \chi_{45}^C, \quad (55)$$

where the pair is created in a color singlet, flavor singlet and spin triplet configuration. The sigma and pion operator as chiral partners, can be written explicitly as [9]

$$\begin{aligned} \text{sigma} &: \mathbf{S}_{4\bar{q}} \cdot (\hat{\mathbf{z}} \times \mathbf{K}_{4\bar{q}}) \\ \text{pion}^a &: \mathbf{S}_{4\bar{q}} \cdot \mathbf{K}_{4\bar{q}} \tau^a \end{aligned} \quad (56)$$

as we also detail in Appendix F, with both carrying the same dimensions and the correct parity assignments. Projecting these structures onto the intrinsic δ coordinate amounts to identifying the transferred momentum with the momentum conjugate to that Jacobi transfer variable, $\mathbf{K}_{4\bar{q}} \rightarrow \frac{4}{\sqrt{3}} \mathbf{k}_\delta$. The effective transition operators are therefore taken in the form

$$\mathcal{T}_\sigma = \frac{1}{2i} \left[\left(S_+^{(4)} + S_+^{(\bar{q})} \right) \frac{4}{\sqrt{5}} k_{\delta,-} - \frac{1}{\sqrt{3}} \chi_{45}^{S_z=+1} - \left(S_-^{(4)} + S_-^{(\bar{q})} \right) \frac{4}{\sqrt{5}} k_{\delta,+} + \frac{1}{\sqrt{3}} \chi_{45}^{S_z=-1} \right], \quad (57)$$

and

$$\begin{aligned} \mathcal{T}_\pi &= \left[\left(S_z^{(4)} + S_z^{(\bar{q})} \right) m_N \frac{(\sqrt{5}x_\sigma - \sqrt{3}x_\gamma) - 1}{2} \frac{1}{\sqrt{3}} \chi_{45}^{S_z=0} \right. \\ &\quad \left. + \frac{1}{2} \left(\left(S_+^{(4)} + S_+^{(\bar{q})} \right) \frac{4}{\sqrt{5}} k_{\delta,-} - \frac{1}{\sqrt{3}} \chi_{45}^{S_z=+1} + \left(S_-^{(4)} + S_-^{(\bar{q})} \right) \frac{4}{\sqrt{5}} k_{\delta,+} + \frac{1}{\sqrt{3}} \chi_{45}^{S_z=-1} \right) \right] \tau^a, \end{aligned} \quad (58)$$

where $k_{\delta,\pm} = k_{\delta,x} \pm ik_{\delta,y} = k_{\delta}e^{\pm i\phi_{\delta}}$ are the transverse circular components in the δ mode. Note that the spin wave function χ_{45} has been included in the above equation to ensure that the quark and anti-quark pair has zero total angular momentum. Equation (57) is the intrinsic realization of the light-front scalar spin-orbit structure $\mathbf{S} \cdot (\hat{z} \times \mathbf{k})$ and therefore excites purely transverse orbital components ($m_L = \pm 1$). In contrast, Eq. (58) is the intrinsic form of $\mathbf{S} \cdot \mathbf{k} \tau^a$ and contains both transverse ($m_L = \pm 1$) and longitudinal ($m_L = 0$) components. However, the operator $S_z^{(4)} + S_z^{(\bar{q})}$ vanish when projected to the zero spin state, so the longitudinal ($m_L = 0$) components in Eq. (58) is zero.

On the light front, it is convenient to express the operator in the Jacobi transverse coordinates. Using the γ - δ variables introduced previously, the transverse σ -type vertex used in the explicit numerical evaluation is written as

$$\begin{aligned} T_{\sigma,\pi}(\vec{k}_{\xi,\perp}, \vec{k}_{\delta,\perp}) &= -3\gamma_0 \delta^2(\vec{k}_{4,\perp} + \vec{k}_{5,\perp}) e^{-r_q^2(\vec{k}_{4,\perp} - \vec{k}_{5,\perp})^2/6} \mathcal{T}_{\sigma,\pi} \chi_{45}^F \chi_{45}^C \\ &= -3\gamma_0 \delta^2 \left(\frac{5\sqrt{3}\vec{k}_{\gamma,\perp} + 3\sqrt{5}\vec{k}_{\delta,\perp}}{10} \right) e^{-r_q^2(\sqrt{5}\vec{k}_{\delta,\perp} - \sqrt{3}\vec{k}_{\gamma,\perp})^2/24} \mathcal{T}_{\sigma,\pi} \chi_{45}^F \chi_{45}^C \\ &= -4\gamma_0 e^{-8r_q^2\vec{k}_{\delta,\perp}^2/15} \mathcal{T}_{\sigma,\pi} \chi_{45}^F \chi_{45}^C \delta^2 \left(\vec{k}_{\gamma,\perp} + \sqrt{\frac{3}{5}}\vec{k}_{\delta,\perp} \right), \end{aligned} \quad (59)$$

with $\gamma_0 = 2.6$ and $r_q = 0.3$ fm in the numerical examples [17].

The key selection rule relevant to the transverse σ -type and π -type mixings are that the orbital part must supply a P -wave in the δ direction in order to saturate the $e^{\pm i\phi_{\delta}}$ factor. This is why, in the explicit evaluation of the transverse mixing matrix element, only the pentaquark orbital representation with $L[4]$ (transverse $m_{\delta} = \pm 1$ components) contributes at leading order, while the $L[31]_{\alpha,\beta,\gamma}$ longitudinal components do not contribute to the same transverse overlap. Therefore, the only pentastate with non-zero mixing with three quark state is $\Psi_{Pm_L}^A$ defined in Eq. (12). The transition matrix element between N and pentastate $\Psi_{Pm_L}^A$ can be expressed as

$$\begin{aligned} \langle N(S_z = \frac{1}{2}) | T_{\sigma,\pi} | P(S_z = \frac{1}{2}) \rangle &= \int [d^2\vec{k}_{\perp,\xi}] [dx_{\xi}] \psi_S^{\dagger}(x'_{\alpha}, x'_{\beta}; k_{\alpha,\perp}, k_{\beta,\perp}) \psi_{L[4]}^1(x_{\alpha}, x_{\beta}, x_{\sigma}, x_{\delta}; k_{\alpha,\perp}, k_{\beta,\perp}, k_{\gamma,\perp}, k_{\delta,\perp}) \\ &\times \frac{1}{\sqrt{3}} \langle SF[3]C[111] | T_{\sigma,\pi}(\vec{k}_{\xi,\perp}, \vec{k}_{\delta,\perp}) | SF[31] ([C[211]_{\beta}SF[31]_{\alpha} - C[211]_{\alpha}SF[31]_{\beta} + C[211]_{\gamma}SF[31]_{\gamma}] C[11]SF[1]) \rangle \end{aligned} \quad (60)$$

where $\psi_S(x; \vec{k}_{\perp})$ represent the light front S wave three quark state obtained by diagonalizing the Hamiltonian given in Appendix D, and x'_{α} and x'_{β} are defined as

$$x'_{\alpha,\beta} = \frac{x_{\alpha,\beta}}{1 - x_4 - x_5} = \frac{10x_{\alpha,\beta}}{5\sqrt{3}x_{\gamma} + 3\sqrt{5}x_{\delta} + 6} \quad (61)$$

The three effective light-front fractions $x'_i(x)$ entering the nucleon wavefunction are obtained from the five-body fractions x_i by removing the total plus momentum carried by the created sigma-pair ¹,

$$X_{\sigma} \equiv x_4 + x_5, \quad 0 < X_{\sigma} < 1, \quad (62)$$

and rescaling the remaining three-quark fractions to unit sum

$$x'_1(x) = \frac{x_1}{1 - X_{\sigma}}, \quad x'_2(x) = \frac{x_2}{1 - X_{\sigma}}, \quad x'_3(x) = \frac{x_3}{1 - X_{\sigma}}. \quad (63)$$

Then one can obtain the corresponding Jacobi coordinates x'_{α} and x'_{β} as shown in Eq. (61). The wave function $\psi_S(x'_{\alpha}, x'_{\beta}; k_{\alpha,\perp}, k_{\beta,\perp})$ expressed in terms of the new variables x' , is normalized to unity.

C. σ -induced and π -induced mixing matrix elements by symmetry channel

For $(I, S) = (\frac{1}{2}, \frac{1}{2})$ the reduced transition elements $\langle N(\frac{1}{2}) | T_{\pi} | P(\frac{1}{2}) \rangle$ and $\langle N(\frac{1}{2}) | T_{\sigma} | P(\frac{1}{2}) \rangle$ in the symmetry basis are listed in Table VII, and for $(I, S) = (\frac{1}{2}, \frac{3}{2})$ they are listed in Table VIII, and the matrix elements

¹ Clearly if $X_{\sigma} = 0$ the overlap would be zero. The created pair carries non-zero longitudinal momentum.

for $(I, S) = (\frac{1}{2}, \frac{5}{2})$ are zero. These values are the direct counterparts of the σ -mixing table, but with a different selection pattern: many channels vanish, and the dominant nonzero entries appear in the symmetry sectors that carry the appropriate longitudinal P -wave content.

D. σ, π mixing summary

The σ -type 3P_0 vertex enforces a strong transverse selection rule: it couples most efficiently to pentaquark configurations that contain an explicit transverse P -wave component in the δ coordinate, thereby isolating the $L[4]$ orbital representation as the dominant contributor to the transverse overlap. After hyperfine diagonalization, this translates into the set of eigenchannels with distinct mixing strengths shown in Table IX.

Although the π -type vertex includes an additional longitudinal coupling, it vanishes due to the spin projection applied to the fourth and fifth quarks. As a result, the corresponding transition matrix elements are very similar to those arising from the σ -type interaction. The vanishing of the $(I, S) = (\frac{1}{2}, \frac{5}{2})$ entries is consistent with the spin constraints built into the operator and the required pair quantum numbers.

These matrix elements enter as off-diagonal blocks that

$$|N_{\text{phys}}, S_z\rangle = \sqrt{Z_N} \left[|N, S_z\rangle + \sum_{n \in \mathcal{P}} C_n^{(\sigma)}(S_z) |P_n, S_z\rangle + \sum_{n \in \mathcal{P}} C_n^{(\pi)}(S_z) |P_n, S_z\rangle \right], \quad (64)$$

where \mathcal{P} is the set of relevant P -wave pentaquark channels (including their (I, S) labels), and Z_N ensures $\langle N_{\text{phys}} | N_{\text{phys}} \rangle = 1$.

A. Perturbative coefficients and energy denominators

Let the unperturbed nucleon mass be $M_N^{(0)}$ and the unperturbed pentaquark eigenenergies be $E_n^{(0)}$ (in the same Hamiltonian scheme used to obtain the hyperfine eigenvectors and spectrum splittings). Denote the energy gaps

$$\Delta_n \equiv E_n^{(0)} - M_N^{(0)}. \quad (65)$$

The $E_n^{(0)}$ includes the spectrum generated by the light cone Hamiltonian, together with the hyper-fine splitting arises from the spin color interaction. The later one can be obtained by diagonalizing the hyper-interactions matrix shown in Table III and IV. The Energy gap between the light cone S wave and P wave state is around 150MeV as shown in the second column in Table VI. Note that only the transverse P components are related in this work since the sigma and pion interactions couple to

mix the lowest nucleon eigenstate with a tower of pentaquark eigenchannels. The relative importance of the σ - and π -induced admixtures then depends on the interplay between: (i) the hyperfine-split pentaquark spectrum, (ii) the orbital overlap suppression factors (transverse for both σ and π), and (iii) the effective couplings γ_0 and the corresponding pion-sector coupling normalization. These ingredients together determine whether a small but non-negligible $qqqq\bar{q}$ component is generated in the physical nucleon state, and which pentaquark symmetry channels dominate that admixture, as we now discuss.

VI. MIXED NUCLEON STATE FROM σ, π TRANSITIONS

We now write the physical nucleon eigenstate in the presence of explicit $qqqq\bar{q}$ admixtures generated by the σ -type (3P_0) and π -type (spin-momentum) transition operators. Following the MSZ logic, we treat the mixing in leading-order degenerate (or quasi-degenerate) perturbation theory: the bare $|N\rangle$ in the three-quark sector mixes with a tower of orthonormal pentaquark eigenchannels $|P_n\rangle$ obtained after hyperfine diagonalization in the five-quark sector. The resulting physical nucleon is then written as a normalized superposition

these transverse modes only. The mass gap between the longitudinal and transverse component is about 150MeV, reflecting the breaking of $O(3)$ symmetry in the light cone frame. The full spectrum of the P state is summarized in Table IX. The parameter $c_0^p = c_0 + 150(\text{MeV})$ with $c_0 = 1756(\text{MeV})$ is an overall parameter by fixing the S wave spectrum in our previous work [16], and additional 150(MeV) is mass gap between light cone S wave and transverse P wave component.

To leading order, the admixture coefficients are

$$C_n^{(\sigma)}(S_z) = \frac{\langle P_n, S_z | T_\sigma | N, S_z \rangle}{\Delta_n},$$

$$C_n^{(\pi)}(S_z) = \frac{\langle P_n, S_z | T_\pi | N, S_z \rangle}{\Delta_n}, \quad (66)$$

with T_σ and T_π defined in Eqs. (57) and (58). The normalization factor is, at the same order,

$$Z_N = 1 - \sum_n \left(|C_n^{(\sigma)}|^2 + |C_n^{(\pi)}|^2 + 2 \text{Re}[C_n^{(\sigma)}(C_n^{(\pi)})^*] \right) + \dots, \quad (67)$$

where the interference term is present if both operators connect $|N\rangle$ to the same orthonormal pentaquark channel $|P_n\rangle$.

	$\langle N, \frac{1}{2} T_\pi v_n, \frac{1}{2} \rangle$	$\langle N, \frac{1}{2} T_\sigma v_n, \frac{1}{2} \rangle$
[4][31] _a	0.0721846 - 0.0416758i	0.0416758 + 0.0721846i
[4][31] _b	0.0721846 - 0.0416758i	0.0416758 + 0.0721846i
[4][31] _c	-0.216554 + 0.125027i	-0.125027 - 0.216554i
[31][31] _a	0	0
[31][31] _b	0	0
[31][31] _c	0	0
[31][22] _a	0	0
[31][22] _b	0	0
[31][4] _a	0	0
[31][4] _b	0	0
[31][211] _a	0	0
[31][211] _b	0	0
[31][211] _c	0	0

TABLE VII: The transition matrix element between the pentastate with $S = \frac{1}{2}$, $I = \frac{1}{2}$ and nucleon state induced by the pion and sigma-type interactions. The numbers in the first and second brackets represent the representation of the orbital angular momentum and spin-flavor. For example, the label [4][31]_a represent the state $L[4]SF[31]_a$ with spin $S = 1/2$ and $I = 1/2$.

	$\langle N, \frac{1}{2} T_\pi v_n, \frac{1}{2} \rangle$	$\langle N, \frac{1}{2} T_\sigma v_n, \frac{1}{2} \rangle$
[4][31] _a	0.204169 - 0.117877i	0.117877 + 0.204169i
[4][31] _b	0.204169 - 0.117877i	0.117877 + 0.204169i
[4][31] _c	0	0
[31][31] _a	0	0
[31][31] _b	0	0
[31][31] _c	0	0
[31][22] _a	0	0
[31][22] _b	0	0
[31][4]	0	0
[31][211] _a	0	0
[31][211] _b	0	0

TABLE VIII: The transition matrix element between the pentastate with $S = \frac{3}{2}$, $I = \frac{1}{2}$ and nucleon state induced by the pion and sigma-type interactions.

B. Explicit σ -induced and π -induced admixture in the hyperfine eigenbasis

For the σ and π operators, we use the orthonormal hyperfine eigenvectors $|P_n\rangle$ to represent the 27 states shown in Table I. The explicit mixed nucleon state with $S_z = \frac{1}{2}$ can be written compactly as

$$|N_{\text{phys}}, \frac{1}{2}\rangle = \sqrt{Z_N} \left[|N, \frac{1}{2}\rangle + \sum_{n=1}^{27} C_n^{(\pi)} \left(\frac{1}{2}\right) |P_n, \frac{1}{2}\rangle + \sum_{n=1}^{27} C_n^{(\sigma)} \left(\frac{1}{2}\right) |P_n, \frac{1}{2}\rangle \right], \quad (68)$$

with

$$C_n^{(\sigma)} \left(\frac{1}{2}\right) = \frac{\langle P_n, \frac{1}{2} | T_\sigma | N, \frac{1}{2} \rangle}{\Delta_n} = \frac{\langle N, \frac{1}{2} | T_\sigma | P_n, \frac{1}{2} \rangle^*}{\Delta_n},$$

$$C_n^{(\pi)} \left(\frac{1}{2}\right) = \frac{\langle P_n, \frac{1}{2} | T_\pi | N, \frac{1}{2} \rangle}{\Delta_n} = \frac{\langle N, \frac{1}{2} | T_\pi | P_n, \frac{1}{2} \rangle^*}{\Delta_n} \quad (69)$$

The coefficients $C_n^{(\sigma)}$ and $C_n^{(\pi)}$ are presented in Table X.

They can be obtained using the results presented in Table IX.

This explicit state is the direct analogue of the MSZ mixed-nucleon wave function: a bare qqq nucleon dressed by a controlled $qqq\bar{q}$ cloud, with the dressing amplitudes determined by microscopic transition operators (σ and π here) and by the hyperfine-resolved five-quark spectrum

	Spectrum1 (color-spin)	$\langle N, \frac{1}{2} T_\pi P, \frac{1}{2} \rangle$	$\langle N, \frac{1}{2} T_\sigma P, \frac{1}{2} \rangle$
$(\frac{1}{2})^+$	$c_0^p - 662.6$	0	0
	$c_0^p - 662.6$	0	0
	$c_0^p - 341.8$	0	0
	$c_0^p - 341.8$	$0.0721846 - 0.0416758i$	$0.0416758 + 0.0721846i$
	$c_0^p - 118.8$	0	0
	$c_0^p - 118.8$	0	0
	$c_0^p - 105.6$	0	0
	$c_0^p - 105.6$	0	0
	$c_0^p - 105.6$	$-0.13347 + 0.0770592i$	$-0.0770592 - 0.13347i$
	$c_0^p + 203.3$	$-0.18518 + 0.106914i$	$-0.106914 - 0.18518i$
	$c_0^p + 203.3$	0	0
	$c_0^p + 203.3$	0	0
	$c_0^p + 537.2$	0	0
	$(\frac{3}{2})^+$	$c_0^p - 219.8$	0
$c_0^p - 219.8$		0	0
$c_0^p - 219.8$		$0.140519 - 0.0811285i$	$0.0811285 + 0.140519i$
$c_0^p - 122.1$		0	0
$c_0^p - 122.1$		0	0
$c_0^p + 24.4$		0	0
$c_0^p + 24.4$		$0.204169 - 0.117877i$	$0.117877 + 0.204169i$
$c_0^p + 244.2$		$-0.14812 + 0.0855169i$	$-0.0855169 - 0.14812i$
$c_0^p + 244.2$		0	0
$c_0^p + 244.2$		0	0
$(\frac{5}{2})^+$	$c_0^p + 244.2$	0	0
	$c_0^p + 244.2$	0	0
	$c_0^p + 244.2$	0	0

TABLE IX: Spectrum lines and transition matrix elements between the nucleon state and P -wave pentaquark eigenstates with $I = \frac{1}{2}$ and spin assignments $\frac{1}{2}^+$, $\frac{3}{2}^+$, $\frac{5}{2}^+$, which are obtained by diagonalizing the matrix of spin color interaction shown in Table III, IV and V. $c_0^p = c_0 + 150(\text{MeV})$ with $c_0 = 1756(\text{MeV})$ is has been determined in our pervious work for S-wave analysis, 150MeV is the mass gap between the first excited state and ground state of light cone Hamiltonian, as shown in Table .VI.

through the energy denominators.

of $P_n^{(\sigma)}$ are

C. Dominant mixing states

Using the coefficients $C_n^{(\sigma)}(\frac{1}{2})$ listed in Table X, we define the probability carried by the n -th hyperfine-diagonalized pentaquark eigenchannel in the physical nucleon in Eq. (68), with the coefficients defined in Eq. (69). In the present case, only 6 out of the 27 P -wave pentastates carry nonzero σ -probability, while the remaining 21 states are exactly null within the accuracy of Table X. This already shows that the σ -induced nucleon dressing is highly sparse and strongly constrained by symmetry. The existence of 27 total P -wave pentastates follows from the counting in Table I: 13 for $S = \frac{1}{2}$, 11 for $S = \frac{3}{2}$, and 3 for $S = \frac{5}{2}$. The canonical OSFC families are $L[4] \otimes SF[31]$, $L[31] \otimes SF[31]$, $L[31] \otimes SF[22]$, $L[31] \otimes SF[4]$, and $L[31] \otimes SF[211]$. The representative flavor \otimes spin irreps relevant for the different total-spin sectors is summarized in Table II.

For the 27 entries shown in Table X, the nonzero values

$$\begin{aligned}
P_4^{(\sigma)} &= 0.01782, \\
P_9^{(\sigma)} &= 0.03209, \\
P_{10}^{(\sigma)} &= 0.03344, \\
P_{16}^{(\sigma)} &= 0.04728, \\
P_{20}^{(\sigma)} &= 0.05664, \\
P_{21}^{(\sigma)} &= 0.01998,
\end{aligned} \tag{70}$$

with all other $P_n^{(\sigma)} = 0$. The largest single contribution is therefore carried by the $n = 20$ eigenchannel, followed by $n = 16$, and then the pair $n = 9, 10$.

To make the sparse structure more transparent, it is useful to isolate only the nonzero contributions and label them by the corresponding symmetry channels. Adopting the natural ordering implied by Table I together with the symmetry-basis ordering in Tables VII and VIII, the

	Spectrum (MeV)	$C_n^{(\sigma)}(\frac{1}{2})$	$C_n^{(\pi)}(\frac{1}{2})$
$(\frac{1}{2})^+$	1243.4	0	0
	1243.4	0	0
	1564.2	0	0
	1564.2	$0.0667703 - 0.11565i$	$0.0667703i + 0.11565$
	1787.2	0	0
	1787.2	0	0
	1800.4	0	0
	1800.4	0	0
	1800.4	$-0.0895611 + 0.155124i$	$-0.0895611i - 0.155124$
	2109.3	$-0.0914374 + 0.158374i$	$-0.0914374i - 0.158374$
	2109.3	0	0
2109.3	0	0	
2443.2	0	0	
$(\frac{3}{2})^+$	1686.25	0	0
	1686.25	0	0
	1686.25	$0.108715 - 0.1883i$	$0.108715i + 0.1883$
	1783.92	0	0
	1783.92	0	0
	1930.42	0	0
	1930.42	$0.119017 - 0.206144i$	$0.119017i + 0.206144$
	2150.17	$-0.0706654 + 0.122396i$	$-0.0706654i - 0.122396$
	2150.17	0	0
$(\frac{5}{2})^+$	2150.2	0	0
	2150.2	0	0
	2150.2	0	0

TABLE X: Spectrum lines and coefficients $C_n^\sigma(\frac{1}{2})$ and $C_n^\pi(\frac{1}{2})$.

six nonzero contributions are assigned as

n	dominant symmetry channel	$P^{(\sigma)}$
4	$[4][31]_b [S = 1/2]$	0.01782
9	$0.585[4][31]_a + 0.811[4][31]_c [S = 1/2]$	0.03209
10	$-0.811[4][31]_a + 0.585[4][31]_c [S = 1/2]$	0.03344
16	$0.688[4][31]_a + 0.725[4][31]_c [S = 3/2]$	0.04728
20	$[4][31]_b [S = 3/2]$	0.05664
21	$-0.725[4][31]_a + 0.688[4][31]_c [S = 3/2]$	0.01998

The first three states are the spin 1/2 states, whereas the last three are spin 3/2 states. This channel assignment should be viewed as the dominant symmetry-channel identification inherited from the basis ordering; after hyperfine diagonalization, each physical eigenstate is in general a linear combination of the underlying OSFC basis states. Nevertheless, the pattern is physically robust: the nonzero strength is concentrated in a very small set of hyperfine-selected channels.

D. Pion-induced admixture and chiral symmetry

The analysis of the π -induced mixing coefficients $C_n^{(\pi)}$ proceeds in complete analogy with the σ case discussed above. In particular, the transition amplitudes are defined by Eq. (69), and the corresponding probabilities

are

$$P_n^{(\pi)} \equiv \left| C_n^{(\pi)}(\frac{1}{2}) \right|^2. \quad (72)$$

A direct inspection of Table VII shows that the pattern of nonzero entries in the π channel is identical to that of the σ channel: only 6 out of the 27 hyperfine eigenstates contribute, while the remaining 21 entries vanish.

This similarity is not accidental, but follows from the underlying chiral structure of the transition operators. The σ -type operator corresponds to a scalar 3P_0 pair-creation vertex, while the π -type operator introduces a spin-momentum coupling associated with pseudoscalar emission. Despite their different Dirac structures, both operators couple the nucleon to the same set of Pauli-allowed pentaquark configurations and share the same selection rules at the level of color-spin-flavor symmetry.

In particular, as noted in Sec. V, the π -type interaction involves an additional longitudinal spin operator, but its contribution vanishes due to the specific spin structure $S_z^{(4)} + S_z^{(\bar{q})}$ acting on the pion state. As a result, the effective transition matrix elements reduce to the same symmetry structure as the σ -induced ones. Consequently, both operators probe the same restricted subset of OSFC channels, leading to identical support in the space of hyperfine eigenstates.

From the perspective of chiral symmetry, this reflects the fact that the σ and π operators form components of a common chiral multiplet. In a light-front Hamiltonian

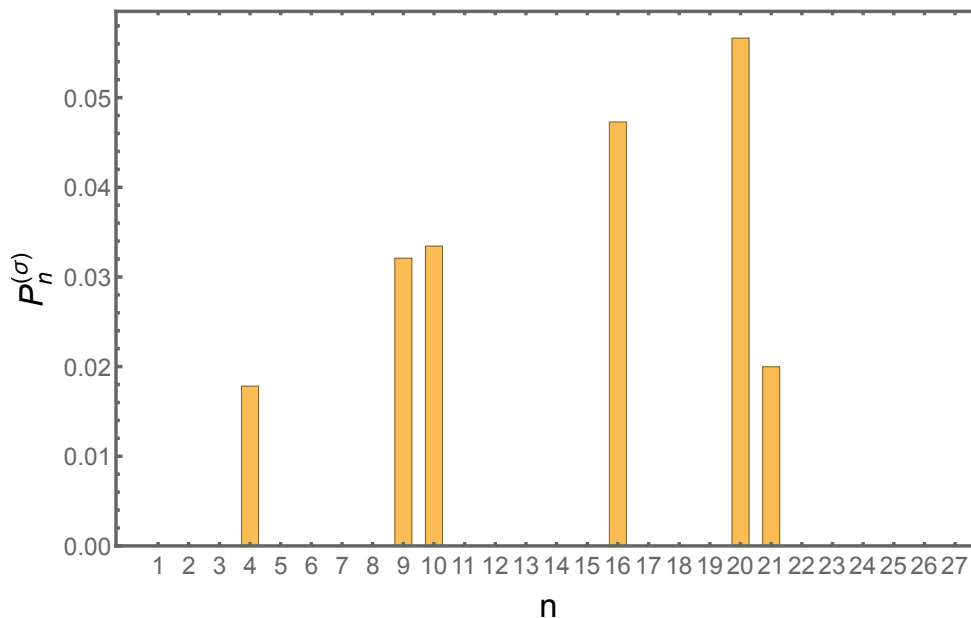


FIG. 1: Histogram of the probabilities $P_n^{(\sigma)} = |C_n^{(\sigma)}|^2$ for the 27 hyperfine-diagonalized P-wave pentastates entering Eq. (64). The distribution is highly sparse: 21 states have vanishing probability, while only 6 states contribute.

framework where the dominant dynamics is governed by color-spin interactions and transverse orbital structure, the distinction between scalar and pseudoscalar couplings is subleading compared to the symmetry constraints imposed by the Pauli principle and the hyperfine Hamiltonian. The observed equality of the support of $P_n^{(\sigma)}$ and $P_n^{(\pi)}$ is therefore a direct manifestation of this underlying chiral structure.

In summary, while the magnitudes of the coefficients $C_n^{(\sigma)}$ and $C_n^{(\pi)}$ may differ at the level of detailed dynamics, the set of contributing pentaquark eigenchannels is identical. This provides a nontrivial consistency check of the framework and confirms that the dominant five-quark admixture in the nucleon is controlled primarily by symmetry selection rules rather than by the specific Dirac structure of the transition operator.

E. Mixing percentages

The total five-quark weight induced by the σ operator is

$$P_{\text{tot}}^{(\sigma)} = \sum_{n=1}^{27} |C_n^{(\sigma)}|^2 = 0.20727, \quad (73)$$

corresponding to about 20.7% at the level of the unnormalized expansion coefficients. Likewise, the π -induced contribution satisfies

$$P_{\text{tot}}^{(\pi)} = \sum_{n=1}^{27} |C_n^{(\pi)}|^2 = 0.20727, \quad (74)$$

since the two operators populate the same set of pentaquark eigenchannels with identical magnitudes.

A crucial simplification arises from the fact that, as seen in Table X, the π -induced coefficients are the complex conjugates of the σ -induced ones,

$$C_n^{(\pi)} = i C_n^{(\sigma)}. \quad (75)$$

As a result, the interference term in Eq. (68) vanishes

$$2 \text{Re} \sum_n C_n^{(\sigma)} \left(C_n^{(\pi)} \right)^* = 0. \quad (76)$$

The total contribution of σ and π interactions become

$$P_{\text{tot}}^{(\sigma+\pi)} = P_{\text{tot}}^{(\sigma)} + P_{\text{tot}}^{(\pi)} = 0.415. \quad (77)$$

The properly normalized five-quark fraction is then

$$P_{5q} = \frac{P_{\text{tot}}^{(\sigma+\pi)}}{1 + P_{\text{tot}}^{(\sigma+\pi)}} \simeq 0.293, \quad (78)$$

corresponding to approximately 29% five-quark content and 71% three-quark core in the physical nucleon.

This result reflects a nontrivial dynamical consequence of the chiral structure of the transition operators: although the σ and π operators individually generate comparable admixtures, their contributions add incoherently.

F. Comparison with recent results

In this subsection we compare our results for nucleon-pentaquark mixing with the recent analysis of five-quark components in the nucleon presented in Ref. [9].

Both works share the common objective of quantifying the role of $qqqq\bar{q}$ configurations in the nucleon wave function and provide further evidence that higher Fock components beyond the three-quark core are phenomenologically significant. In particular, both approaches identify dynamical mechanisms that generate mixing between $|qqq\rangle$ and $|qqqq\bar{q}\rangle$ sectors and find that the resulting five-quark probability is sizable, at the level of $\mathcal{O}(10\% - 30\%)$. This agreement supports the general picture that nucleon structure is intrinsically multi-partonic.

The two analyses differ qualitatively in how symmetry and dynamics constrain the mixing pattern. A primary distinction lies in the implementation of the Pauli principle. In the present work, the four-quark core is constructed using a complete S_4 permutation-group classification, ensuring that the combined orbital, spin-flavor, and color wave function is fully antisymmetric and free of redundancies. This leads to exact selection rules at the level of the basis itself. As a direct consequence, only 6 out of the 27 positive-parity P -wave pentastates contribute to nucleon mixing, while the remaining 21 vanish identically. The resulting sparsity is therefore not a dynamical accident but a symmetry-enforced constraint.

In contrast, Ref. [9] does not organize the five-quark basis in terms of a complete S_4 classification, but uses instead a large monom basis ($4 \times 3^6 \times 2^5 \times 2^5$) to diagonalize the S_4 permutation group with extensive use of Mathematica. As a result, the Pauli constraints are implemented less explicitly, and a larger set of configurations can contribute to the mixing. This leads to a more distributed pattern of amplitudes in which the underlying symmetry selection rules are less transparent, and the effective number of contributing channels is significantly larger.

Additionally, there is a slight difference in the structure of the transition operators. In our light-front Hamiltonian framework, the σ - and π -type operators form a chiral pair and act on the same restricted set of Pauli-allowed configurations. Their amplitudes are related by a fixed phase,

$$C_n^{(\pi)} = i C_n^{(\sigma)}, \quad (79)$$

which implies that the interference term vanishes exactly in the normalization. The two contributions therefore add incoherently, leading to a tightly constrained and correlated pattern of mixing.

Finally, in the present work, hyperfine color-spin interactions are diagonalized explicitly in the full symmetry-adapted basis, yielding orthonormal eigenchannels that reorganize the original configurations into physically meaningful states. The mixing is then expressed in this eigenbasis, which reveals a clear hierarchy in which only a small number of eigenchannels dominate the five-quark admixture. In contrast, analyses that do not perform a full hyperfine diagonalization typically work in a fixed configuration basis, where the strength is distributed more broadly and the identification of dominant structures is less direct.

These differences lead to a qualitatively distinct interpretation of the five-quark content of the nucleon. In the present work, the result

$$P_{5q} \simeq 29\%, \quad (80)$$

emerges from a highly sparse and symmetry-selected set of channels, dominated by a few hyperfine eigenstates. This indicates that the five-quark component is not a superposition of many configurations, but rather a structured admixture controlled by symmetry selection rules and chiral dynamics. The comparison therefore highlights the importance of implementing exact permutation symmetry, together with chiral operator structure and hyperfine diagonalization, in order to reveal the underlying organization of higher Fock components in baryons.

VII. CONCLUSIONS

In this work we have carried out a systematic light-front Hamiltonian analysis of nucleon-pentaquark mixing induced by σ - and π -type transition operators in a fully Pauli-consistent five-quark basis. Using a permutation-group construction of the orbital, spin-flavor, and color degrees of freedom, we have built a complete set of positive-parity P -wave pentaquark states and organized them into symmetry-adapted bases suitable for dynamical calculations. The inclusion of hyperfine color-spin interactions and their diagonalization yields a set of orthonormal eigenchannels that provide a physically meaningful description of the five-quark sector.

A central result of this analysis is the emergence of strong symmetry selection rules that drastically reduce the effective number of contributing channels. Among the 27 possible P -wave pentastates, only 6 contribute to the physical nucleon state, while the remaining 21 vanish identically. The resulting five-quark admixture is therefore highly sparse and dominated by a small number of hyperfine-selected channels. Furthermore, we have shown that the σ - and π -induced amplitudes populate the same subset of states and are related by complex conjugation, reflecting their common chiral structure. After normalization, the nucleon contains a five-quark component of approximately 29%, with the remainder residing in the three-quark core.

Beyond these specific results, an important outcome of this work is the explicit construction of the mixed nucleon wave function in a fully symmetry-controlled framework. The expressions given in Sec. VI, together with the tabulated coefficients in Table X, provide a concrete and reusable representation of the nucleon state including its five-quark components. In this sense, the present work serves as a repository of the mixed nucleon wave function, suitable for future theoretical and phenomenological applications and for cross-checks with alternative approaches.

The availability of this explicit wave function opens several directions for further study. The five-quark com-

ponents provide a natural framework for analyzing flavor asymmetries in the nucleon sea, including the $\bar{d}-\bar{u}$ imbalance and possible strange-quark contributions. They also encode nontrivial orbital structure, offering a pathway to quantifying orbital angular momentum contributions to the nucleon spin. In addition, the mixed wave function can be used to compute static and dynamical observables such as magnetic moments and transition form factors, as well as more differential quantities including generalized parton distributions (GPDs) and transverse-momentum-dependent distributions (TMDs). In all these cases, the strong symmetry selection rules identified here imply that only a small subset of channels will dominate the physical observables.

More broadly, the framework developed here provides a bridge between symmetry-based constructions of hadronic wave functions and dynamical light-front calculations. The combination of Pauli-consistent basis states, controlled transition operators, and hyperfine dynamics offers a systematic approach to incorporating higher Fock components in baryon structure. The resulting picture is one in which nucleon–pentaquark mixing is governed primarily by symmetry and chiral structure, leading to a reduced and highly organized five-quark content that can be quantitatively explored in future studies.

VIII. ACKNOWLEDGEMENTS

This work is supported by the Office of Science, U.S. Department of Energy under Contract No. DE-FG-88ER40388. FH is supported by the U.S. Department of Energy, Office of Science, Office of Nuclear Physics, under Grant No. DE-SC0013065. This research is also supported in part within the framework of the Quark-Gluon Tomography (QGT) Topical Collaboration, under contract no. DE-SC0023646.

Appendix A: S_3 tensor-product projections and cluster recoupling

Although the pentaquark core is governed by S_4 , S_3 enters whenever one isolates a three-quark cluster or performs intermediate couplings. The simplest couplings serve as consistency checks and define phase conventions.

Coupling two symmetric irreps yields

$$[3]_A \otimes [3]_B = [3]_{AB}, \quad ([3]_{AB} : [3]_A \otimes [3]_B) = A[3] B[3]. \quad (\text{A1})$$

Coupling a symmetric with a mixed irrep gives

$$[3]_A \otimes [21]_B = [21]_{AB}, \quad ([21]_{AB} : [3]_A \otimes [21]_B)_{\alpha,\beta} = A[3] B[21]_{\alpha,\beta}. \quad (\text{A2})$$

The nontrivial case is $[21] \otimes [21]$, which contains all three irreps:

$$[21]_A \otimes [21]_B = [3]_{AB} \oplus [21]_{AB} \oplus [111]_{AB}. \quad (\text{A3})$$

The explicit projections are

$$\begin{aligned} ([3]_{AB} : [21]_A \otimes [21]_B) &= \frac{1}{\sqrt{2}} \left(A[21]_{\alpha} B[21]_{\alpha} + A[21]_{\beta} B[21]_{\beta} \right), \\ ([111]_{AB} : [21]_A \otimes [21]_B) &= \frac{1}{\sqrt{2}} \left(A[21]_{\alpha} B[21]_{\beta} - A[21]_{\beta} B[21]_{\alpha} \right), \\ ([21]_{AB} : [21]_A \otimes [21]_B)_{\alpha} &= \frac{1}{\sqrt{2}} \left(A[21]_{\alpha} B[21]_{\beta} + A[21]_{\beta} B[21]_{\alpha} \right), \\ ([21]_{AB} : [21]_A \otimes [21]_B)_{\beta} &= \frac{1}{\sqrt{2}} \left(A[21]_{\alpha} B[21]_{\alpha} - A[21]_{\beta} B[21]_{\beta} \right). \end{aligned} \quad (\text{A4})$$

In physical terms, the first line isolates the exchange-even component of the product, the second isolates the exchange-odd component, and the last two span the mixed irrep. These are precisely the combinations that appear, for example, when two mixed-symmetry subsystems are coupled to produce a symmetric (or antisymmetric) effective cluster state.

Appendix B: S_4 tensor-product projections for the four-quark core

For four identical quarks the permutation group is S_4 , and the relevant irreducible representations are $[4]$, $[31]$, $[22]$, $[211]$, and $[1111]$. The Pauli principle requires that the total four-quark wave function transform as $[1111]$ under S_4 . Writing the four-quark wave function as a product of orbital, spin-flavor, and color factors, this con-

straint becomes

$$[f_{\text{orb}}] \otimes [f_{\text{SF}}] \otimes [f_{\text{color}}] \supset [1111]. \quad (\text{B1})$$

This single condition determines which combinations of orbital excitation, color structure, and spin-flavor symmetry are allowed.

We now list the S_4 projections required to couple symmetry types across different physical factors of the four-quark core. The simplest products involve a totally symmetric factor. Since [4] is the identity representation of S_4 in the sense of tensoring, it leaves the other symmetry type unchanged

$$[4]_A \otimes [4]_B = [4]_{AB}, \quad ([4]_{AB} : [4]_A \otimes [4]_B) = A[4] B[4], \quad (\text{B2})$$

$$[4]_A \otimes [31]_B = [31]_{AB}, \quad ([31]_{AB} : [4]_A \otimes [31]_B)_\alpha = A[4] B[31]_\alpha, \quad (\text{B3})$$

$$[4]_A \otimes [22]_B = [22]_{AB}, \quad ([22]_{AB} : [4]_A \otimes [22]_B)_\alpha = A[4] B[22]_\alpha, \quad (\text{B4})$$

$$[4]_A \otimes [211]_B = [211]_{AB}, \quad ([211]_{AB} : [4]_A \otimes [211]_B)_\alpha = A[4] B[211]_\alpha. \quad (\text{B5})$$

These relations are heavily used when the orbital part is taken in its lowest configuration [4] and one wishes to infer that the entire symmetry bookkeeping is carried by color and spin-flavor.

The workhorse decomposition in many pentaquark channels is $[31] \otimes [31]$. It arises, for example, when both orbital and spin-flavor parts are of [31] type (a common situation for negative-parity states built from a single P -wave excitation together with a mixed-symmetry spin-flavor core), or when color is in a mixed irrep and must be combined with another mixed factor to reach [1111]. The decomposition is

$$[31]_A \otimes [31]_B = [4]_{AB} \oplus [31]_{AB} \oplus [22]_{AB} \oplus [211]_{AB}, \quad (\text{B6})$$

and the explicit normalized projections read

$$\begin{aligned} ([4]_{AB} : [31]_A \otimes [31]_B) &= \frac{1}{\sqrt{3}} \left(A[31]_\alpha B[31]_\alpha + A[31]_\beta B[31]_\beta + A[31]_\gamma B[31]_\gamma \right), \\ ([31]_{AB} : [31]_A \otimes [31]_B)_\alpha &= \frac{1}{\sqrt{3}} \left(A[31]_\alpha B[31]_\beta + A[31]_\beta B[31]_\alpha \right) + \frac{1}{\sqrt{6}} \left(A[31]_\alpha B[31]_\gamma + A[31]_\gamma B[31]_\alpha \right), \\ ([31]_{AB} : [31]_A \otimes [31]_B)_\beta &= \frac{1}{\sqrt{3}} \left(A[31]_\alpha B[31]_\alpha - A[31]_\beta B[31]_\beta \right) + \frac{1}{\sqrt{6}} \left(A[31]_\gamma B[31]_\beta + A[31]_\beta B[31]_\gamma \right), \\ ([31]_{AB} : [31]_A \otimes [31]_B)_\gamma &= \frac{1}{\sqrt{6}} \left(A[31]_\alpha B[31]_\alpha + A[31]_\beta B[31]_\beta \right) - \frac{2}{\sqrt{6}} A[31]_\gamma B[31]_\gamma, \\ ([22]_{AB} : [31]_A \otimes [31]_B)_\alpha &= \frac{1}{\sqrt{6}} \left(A[31]_\alpha B[31]_\beta + A[31]_\beta B[31]_\alpha \right) - \frac{1}{\sqrt{3}} \left(A[31]_\alpha B[31]_\gamma + A[31]_\gamma B[31]_\alpha \right), \\ ([22]_{AB} : [31]_A \otimes [31]_B)_\beta &= \frac{1}{\sqrt{6}} \left(A[31]_\alpha B[31]_\alpha - A[31]_\beta B[31]_\beta \right) - \frac{1}{\sqrt{3}} \left(A[31]_\beta B[31]_\gamma + A[31]_\gamma B[31]_\beta \right), \\ ([211]_{AB} : [31]_A \otimes [31]_B)_\alpha &= \frac{A[31]_\alpha B[31]_\gamma - A[31]_\gamma B[31]_\alpha}{\sqrt{2}}, \\ ([211]_{AB} : [31]_A \otimes [31]_B)_\beta &= \frac{A[31]_\beta B[31]_\gamma - A[31]_\gamma B[31]_\beta}{\sqrt{2}}, \\ ([211]_{AB} : [31]_A \otimes [31]_B)_\gamma &= \frac{A[31]_\alpha B[31]_\beta - A[31]_\beta B[31]_\alpha}{\sqrt{2}}. \end{aligned} \quad (\text{B7})$$

A useful physical way to read these expressions is the following. The [4] projector extracts the ‘‘aligned’’ combination where the basis labels match ($\alpha\alpha + \beta\beta + \gamma\gamma$), i.e. the maximally symmetric component. The [211] projectors are manifestly antisymmetric under interchange of $A \leftrightarrow B$ in the paired basis labels, reflecting the deeper antisymmetry content of [211]. The remaining [31] and [22] combinations interpolate between these extremes and correspond to distinct Pauli-allowed recouplings.

The coupling $[31] \otimes [22]$ arises whenever a pair-symmetry structure ([22]) must be combined with a one-quark-distinguished structure ([31]), as happens in diquark-motivated bases or when mixing channels with different internal clusterizations. One has

$$[31]_A \otimes [22]_B = [31]_{AB} \oplus [211]_{AB}, \quad (\text{B8})$$

with

$$\begin{aligned}
([31]_{AB} : [31]_A \otimes [22]_B)_\alpha &= \frac{1}{2} \left(B[22]_\alpha A[31]_\beta + B[22]_\beta A[31]_\alpha \right) - \frac{1}{\sqrt{2}} B[22]_\alpha A[31]_\gamma, \\
([31]_{AB} : [31]_A \otimes [22]_B)_\beta &= \frac{1}{2} \left(B[22]_\alpha A[31]_\alpha - B[22]_\beta A[31]_\beta \right) - \frac{1}{\sqrt{2}} B[22]_\beta A[31]_\gamma, \\
([31]_{AB} : [31]_A \otimes [22]_B)_\gamma &= -\frac{1}{\sqrt{2}} \left(B[22]_\alpha A[31]_\alpha + B[22]_\beta A[31]_\beta \right), \\
([211]_{AB} : [31]_A \otimes [22]_B)_\alpha &= \frac{A[31]_\alpha B[22]_\beta + A[31]_\beta B[22]_\alpha + \sqrt{2} A[31]_\gamma B[22]_\alpha}{2}, \\
([211]_{AB} : [31]_A \otimes [22]_B)_\beta &= \frac{A[31]_\alpha B[22]_\alpha - A[31]_\beta B[22]_\beta + \sqrt{2} A[31]_\gamma B[22]_\beta}{2}, \\
([211]_{AB} : [31]_A \otimes [22]_B)_\gamma &= \frac{A[31]_\alpha B[22]_\beta - A[31]_\beta B[22]_\alpha}{\sqrt{2}}.
\end{aligned} \tag{B9}$$

Here the appearance of both symmetric and antisymmetric combinations is again the group-theoretic manifestation of whether the resulting coupling can participate in an overall antisymmetric four-quark state.

The product $[31] \otimes [211]$ is important when one factor already contains substantial antisymmetry and must be coupled to a mixed factor. It decomposes as

$$[31]_A \otimes [211]_B = [31]_{AB} \oplus [22]_{AB} \oplus [211]_{AB} \oplus [1111]_{AB}. \tag{B10}$$

In pentaquark applications, the explicit appearance of $[1111]$ in this product is especially valuable: it provides a direct route to a Pauli-allowed core when the remaining factor is symmetric. The projections are

$$\begin{aligned}
([31]_{AB} : [31]_A \otimes [211]_B)_\alpha &= \frac{A[31]_\gamma B[211]_\alpha + A[31]_\beta B[211]_\gamma}{\sqrt{2}}, \\
([31]_{AB} : [31]_A \otimes [211]_B)_\beta &= \frac{A[31]_\gamma B[211]_\beta - A[31]_\alpha B[211]_\gamma}{\sqrt{2}}, \\
([31]_{AB} : [31]_A \otimes [211]_B)_\gamma &= \frac{-A[31]_\alpha B[211]_\alpha - A[31]_\beta B[211]_\beta}{\sqrt{2}}, \\
([22]_{AB} : [31]_A \otimes [211]_B)_\alpha &= \frac{1}{\sqrt{6}} \left(A[31]_\alpha B[211]_\beta + A[31]_\beta B[211]_\alpha \right) - \frac{1}{\sqrt{3}} \left(A[31]_\beta B[211]_\gamma - A[31]_\gamma B[211]_\alpha \right), \\
([22]_{AB} : [31]_A \otimes [211]_B)_\beta &= \frac{1}{\sqrt{6}} \left(A[31]_\alpha B[211]_\alpha - A[31]_\beta B[211]_\beta \right) + \frac{1}{\sqrt{3}} \left(A[31]_\alpha B[211]_\gamma + A[31]_\gamma B[211]_\beta \right), \\
([211]_{AB} : [31]_A \otimes [211]_B)_\alpha &= \frac{1}{\sqrt{3}} \left(A[31]_\alpha B[211]_\beta + A[31]_\beta B[211]_\alpha \right) + \frac{1}{\sqrt{6}} \left(A[31]_\beta B[211]_\gamma - A[31]_\gamma B[211]_\alpha \right), \\
([211]_{AB} : [31]_A \otimes [211]_B)_\beta &= \frac{1}{\sqrt{3}} \left(A[31]_\alpha B[211]_\alpha - A[31]_\beta B[211]_\beta \right) - \frac{1}{\sqrt{6}} \left(A[31]_\alpha B[211]_\gamma + A[31]_\gamma B[211]_\beta \right), \\
([211]_{AB} : [31]_A \otimes [211]_B)_\gamma &= -\frac{1}{\sqrt{6}} \left(A[31]_\alpha B[211]_\beta - A[31]_\beta B[211]_\alpha \right) + \frac{2}{\sqrt{6}} A[31]_\gamma B[211]_\gamma, \\
([1111]_{AB} : [31]_A \otimes [211]_B) &= \frac{1}{\sqrt{3}} \left(A[31]_\alpha B[211]_\beta - A[31]_\beta B[211]_\alpha + A[31]_\gamma B[211]_\gamma \right).
\end{aligned} \tag{B11}$$

The remaining products are included for completeness and for later use in channel mixing, where operators can connect basis states built from different internal symmetry couplings.

The product $[22] \otimes [22]$ decomposes as

$$[22]_A \otimes [22]_B = [4]_{AB} \oplus [22]_{AB} \oplus [1111]_{AB}, \tag{B12}$$

with projections

$$\begin{aligned}
([4]_{AB} : [22]_A \otimes [22]_B) &= \frac{1}{\sqrt{2}} \left(A[22]_\alpha B[22]_\alpha + A[22]_\beta B[22]_\beta \right), \\
([22]_{AB} : [22]_A \otimes [22]_B)_\alpha &= \frac{1}{\sqrt{2}} \left(A[22]_\alpha B[22]_\beta + A[22]_\beta B[22]_\alpha \right), \\
([22]_{AB} : [22]_A \otimes [22]_B)_\beta &= \frac{1}{\sqrt{2}} \left(A[22]_\alpha B[22]_\alpha - A[22]_\beta B[22]_\beta \right), \\
([1111]_{AB} : [22]_A \otimes [22]_B) &= \frac{1}{\sqrt{2}} \left(A[22]_\alpha B[22]_\beta - A[22]_\beta B[22]_\alpha \right).
\end{aligned} \tag{B13}$$

The appearance of [1111] here is another direct mechanism to build an antisymmetric four-quark state from pairwise correlated structures, which is why [22]-based diquark pictures can be compatible with Pauli constraints if the remaining factors are arranged appropriately.

The product $[22] \otimes [211]$ yields

$$[22]_A \otimes [211]_B = [31]_{AB} \oplus [211]_{AB}, \tag{B14}$$

with

$$\begin{aligned}
([31]_{AB} : [22]_A \otimes [211]_B)_\alpha &= \frac{1}{2} \left(A[22]_\alpha B[211]_\beta + A[22]_\beta B[211]_\alpha \right) + \frac{1}{\sqrt{2}} A[22]_\beta B[211]_\gamma, \\
([31]_{AB} : [22]_A \otimes [211]_B)_\beta &= \frac{1}{2} \left(A[22]_\alpha B[211]_\alpha - A[22]_\beta B[211]_\beta \right) - \frac{1}{\sqrt{2}} A[22]_\alpha B[211]_\gamma, \\
([31]_{AB} : [22]_A \otimes [211]_B)_\gamma &= \frac{1}{\sqrt{2}} \left(A[22]_\alpha B[211]_\alpha + A[22]_\beta B[211]_\beta \right), \\
([211]_{AB} : [22]_A \otimes [211]_B)_\alpha &= \frac{1}{2} \left(A[22]_\alpha B[211]_\beta + A[22]_\beta B[211]_\alpha \right) - \frac{1}{\sqrt{2}} A[22]_\beta B[211]_\gamma, \\
([211]_{AB} : [22]_A \otimes [211]_B)_\beta &= \frac{1}{2} \left(A[22]_\alpha B[211]_\alpha - A[22]_\beta B[211]_\beta \right) + \frac{1}{\sqrt{2}} A[22]_\alpha B[211]_\gamma, \\
([211]_{AB} : [22]_A \otimes [211]_B)_\gamma &= \frac{1}{\sqrt{2}} \left(A[22]_\alpha B[211]_\beta - A[22]_\beta B[211]_\alpha \right).
\end{aligned} \tag{B15}$$

In later use, these relations control how pairwise symmetry in one factor (e.g. orbital) correlates with antisymmetry content in another (e.g. color).

Finally, the product $[211] \otimes [211]$ decomposes as

$$[211]_A \otimes [211]_B = [4]_{AB} \oplus [31]_{AB} \oplus [22]_{AB} \oplus [211]_{AB}, \tag{B16}$$

with

$$\begin{aligned}
([4]_{AB} : [211]_A \otimes [211]_B) &= \frac{1}{\sqrt{3}} \left(A[211]_\alpha B[211]_\alpha + A[211]_\beta B[211]_\beta + A[211]_\gamma B[211]_\gamma \right), \\
([31]_{AB} : [211]_A \otimes [211]_B)_\alpha &= \frac{1}{\sqrt{6}} \left(A[211]_\alpha B[211]_\beta + A[211]_\beta B[211]_\alpha \right) - \frac{1}{\sqrt{3}} \left(A[211]_\beta B[211]_\gamma + A[211]_\gamma B[211]_\beta \right), \\
([31]_{AB} : [211]_A \otimes [211]_B)_\beta &= \frac{1}{\sqrt{6}} \left(A[211]_\alpha B[211]_\alpha - A[211]_\beta B[211]_\beta \right) + \frac{1}{\sqrt{3}} \left(A[211]_\alpha B[211]_\gamma + A[211]_\gamma B[211]_\alpha \right), \\
([31]_{AB} : [211]_A \otimes [211]_B)_\gamma &= -\frac{1}{\sqrt{6}} \left(A[211]_\alpha B[211]_\alpha + A[211]_\beta B[211]_\beta \right) + \frac{2}{\sqrt{6}} A[211]_\gamma B[211]_\gamma, \\
([22]_{AB} : [211]_A \otimes [211]_B)_\alpha &= \frac{1}{\sqrt{6}} \left(A[211]_\alpha B[211]_\beta + A[211]_\beta B[211]_\alpha \right) + \frac{1}{\sqrt{3}} \left(A[211]_\beta B[211]_\gamma + A[211]_\gamma B[211]_\beta \right), \\
([22]_{AB} : [211]_A \otimes [211]_B)_\beta &= \frac{1}{\sqrt{6}} \left(A[211]_\alpha B[211]_\alpha - A[211]_\beta B[211]_\beta \right) - \frac{1}{\sqrt{3}} \left(A[211]_\alpha B[211]_\gamma + A[211]_\gamma B[211]_\alpha \right), \\
([211]_{AB} : [211]_A \otimes [211]_B)_\alpha &= \frac{1}{\sqrt{2}} \left(A[211]_\beta B[211]_\gamma - A[211]_\gamma B[211]_\beta \right), \\
([211]_{AB} : [211]_A \otimes [211]_B)_\beta &= -\frac{1}{\sqrt{2}} \left(A[211]_\alpha B[211]_\gamma - A[211]_\gamma B[211]_\alpha \right), \\
([211]_{AB} : [211]_A \otimes [211]_B)_\gamma &= \frac{1}{\sqrt{2}} \left(A[211]_\alpha B[211]_\beta - A[211]_\beta B[211]_\alpha \right).
\end{aligned} \tag{B17}$$

Appendix C: Light-front P -wave pentaquark orbital states

A five-parton $qqqq\bar{q}$ light-front state is described by longitudinal momentum fractions x_i and transverse momenta $\mathbf{k}_{i\perp}$ with

$$\sum_{i=1}^5 x_i = 1, \quad x_i \geq 0, \quad \sum_{i=1}^5 \mathbf{k}_{i\perp} = 0, \tag{C1}$$

together with internal spin-flavor-color quantum numbers. The orbital content on the light front is organized by the conserved projection L_z generated by transverse rotations,

$$L_z = -i \sum_{i=1}^5 \frac{\partial}{\partial \varphi_i}, \tag{C2}$$

where φ_i is the azimuthal angle of $\mathbf{k}_{i\perp}$. It is convenient to use $k_\perp^\pm = k_x \pm ik_y \propto e^{\pm i\varphi}$ so that a single factor of k_\perp^\pm carries $L_z = \pm 1$ and therefore implements the transverse members of a P -wave multiplet.

To separate the internal motion we introduce four longitudinal momenta using Jacobi momenta $x_{\alpha,\beta,\gamma,\delta}$ in the center-of-momentum frame, chosen so that α, β, γ resolve the internal motion of the q^4 core while δ resolves the relative motion of the q^4 subsystem with respect to the antiquark. A convenient explicit choice for the longitudinal

part,

$$\begin{aligned}
x_\alpha &= \frac{x_1 - x_2}{\sqrt{2}}, \\
x_\beta &= \frac{x_1 + \sqrt{2}x_2 - 2x_3}{\sqrt{6}}, \\
x_\gamma &= \frac{x_1 + x_2 + x_3 - 3x_4}{\sqrt{12}}, \\
x_\delta &= \frac{x_1 + x_2 + x_3 + x_4 - 4x_5}{\sqrt{20}}
\end{aligned} \tag{C3}$$

where 1, 2, 3, 4 label the identical quarks and 5 labels the antiquark. The transverse Jacobi coordinates can be defined similarly. The final expression for the light front Hamiltonian, free of CM, is then given by [16]

$$\begin{aligned}
H_{LF} &\equiv \sum_{i=1}^5 \frac{k_{i\perp}^2 + m_Q^2}{x_i} + 5\sigma_T a \\
&- \frac{\sigma_T}{a} \sum_{\xi=\alpha,\beta,\gamma,\delta} ((\partial/\partial x_\xi)^2 + M^2(\partial/\partial \vec{k}_{\xi\perp})^2)
\end{aligned} \tag{C4}$$

where $a = 7.59$ has been determined by minimizing the ground state mass [16]. To diagonalize the Light front Hamiltonian in Eq. (C4), one needs to find the proper basis. For the longitudinal part, we use the complete and orthogonal basis constructed using Slater determinants [16],

$$\varphi_{\tilde{n}}[N=5] = \frac{1}{5^{3/4}} \begin{vmatrix} 1 & 1 & \dots & 1 \\ e^{i\tilde{n}_{21}\tilde{s}_1} & e^{i\tilde{n}_{21}\tilde{s}_2} & \dots & e^{i\tilde{n}_{21}\tilde{s}_5} \\ \vdots & \vdots & \ddots & \vdots \\ e^{i\tilde{n}_{51}\tilde{s}_1} & e^{i\tilde{n}_{51}\tilde{s}_2} & \dots & e^{i\tilde{n}_{51}\tilde{s}_5} \end{vmatrix} \quad (\text{C5})$$

with

$$\begin{aligned} \tilde{s}_1 &= \frac{1}{10} \left(2\sqrt{5}x_\delta + 2\sqrt{3}x_\gamma + 4 + \sqrt{2}x_\alpha + \sqrt{6}x_\beta \right) \\ \tilde{s}_2 &= \frac{1}{30} \left(-12\sqrt{2}x_\alpha - 2\sqrt{6}x_\beta + 3\sqrt{5}x_\delta + \sqrt{3}x_\gamma + 6 \right) \\ \tilde{s}_3 &= \frac{1}{30} \left(3\sqrt{2}x_\alpha - 7\sqrt{6}x_\beta - 4\sqrt{3}x_\gamma \right) \\ \tilde{s}_4 &= \frac{1}{10} \left(\sqrt{2}x_\alpha + \sqrt{6}x_\beta - \sqrt{5}x_\delta - 3\sqrt{3}x_\gamma - 2 \right) \\ \tilde{s}_5 &= \frac{1}{10} \left(-2\sqrt{5}x_\delta + 2\sqrt{3}x_\gamma - 4 + \sqrt{2}x_\alpha + \sqrt{6}x_\beta \right) \end{aligned} \quad (\text{C6})$$

Note that the correct normalization factor is $\frac{1}{5^{3/4}}$, the factor $\frac{1}{5^{4/3}}$ given in our previous paper [16] was a typo and does not effect any numerical results presented in

[16]. The coefficients \tilde{n}_{i1} are ordered as $0 < \tilde{n}_{21} < \tilde{n}_{31} < \tilde{n}_{41} \dots$ to avoid repeated counting of the same state. The eigenfunctions used for the each transverse component are of generalized Laguerre polynomials,

$$\psi_{n,m}^\perp(k_{\xi\perp}, \beta) = \frac{1}{\sqrt{\pi}} \beta^{1/4} \sqrt{\frac{n!}{(n+|m|)!}} e^{-\frac{k_{\xi\perp}^2 \beta^{1/2}}{2} + im\phi} (k_{\xi\perp} \beta^{1/4})^{|m|} L_n^{|m|}(\beta^{1/2} k_{\xi\perp}^2) \quad (\text{C7})$$

with $\beta = 5a/(\sigma_T M^2)$ and and eigenvalues

$$E_{n,m} = 2\sqrt{5}(\sigma_T M^2/a)^{1/2}(2n + |m| + 1).$$

Note that the basis in Eq. (C7). $\xi = \alpha, \beta, \gamma, \delta$ represent the different Jacobi components, the total transverse eigenfunctions are the product of $\psi_{n,m}^\perp(k_{\xi\perp}, \beta)$ over four

Jacobi components.

In the rest frame, a minimal P -shell orbital basis with definite S_4 symmetry for the four identical quarks is spanned by the totally symmetric irrep $L[4]$ and the mixed irrep $L[31]$, expressed on one Jacobi direction,

$$\begin{aligned} L[4](L_z = \pm 1) &\propto e^{\pm i\phi_\delta}, & L[31]_\alpha(L_z = \pm 1) &\propto e^{\pm i\phi_\alpha}, & L[31]_\beta(L_z = \pm 1) &\propto e^{\pm i\phi_\beta}, & L[31]_\gamma(L_z = \pm 1) &\propto e^{\pm i\phi_\gamma}, \\ L[4](L_z = 0) &\propto x_\delta, & L[31]_\alpha(L_z = 0) &\propto x_\alpha, & L[31]_\beta(L_z = 0) &\propto x_\beta, & L[31]_\gamma(L_z = 0) &\propto x_\gamma, \end{aligned} \quad (\text{C8})$$

which furnish the [4] and [31] irreps of S_4 when combined with the appropriate S_4 projection relations among the [31] basis vectors. The components with $L_z = \pm 1$ are related to the rotation angular in the transverse direction. The component with $L_z = 0$ is related to the longitudinal momentum.

The numbers of eigenfunction used to diagonalize the light cone Hamiltonian are very huge since we need multiply the longitudinal basis and transverse basis over four Jacobi coordinates once we combine different choices of

(n, m) satisfies the truncation condition. In this calculation, we set the index $m = \pm 1, 0$ in Eq. (C7) for the δ coordinate, and $m = 0$ for other Jacobi coordinates since the sigma- and pion-type interactions shown in Eq. (57) and Eq. (58) contain only the $e^{\pm i\phi_\delta}$ component. The longitudinal and transverse eigen-sets are truncated using the following constraints

$$E_L = \sum_{i=2}^5 \tilde{n}_{i1}^2 - \frac{1}{5} \left(\sum_{i=2}^5 \tilde{n}_{i1} \right)^2 \leq \frac{1184\pi^2}{5},$$

$$E_T = \sum_{i=1}^4 (2n_i + |m|_i + 1) \leq 10, \quad (\text{C9})$$

In practical LF Hamiltonian diagonalizations one often obtains orthonormal five-body eigenstates $\psi_n(x, \mathbf{k}_\perp)$ and then reconstructs the symmetry-adapted orbital content by projection. For the $L[4]$ transverse sector one projects onto the azimuthal phase of the δ Jacobi transverse momentum, while for the $L[31]$ longitudinal sector one projects onto the longitudinal Jacobi coordinates, as shown in Eq. (C8), enforcing orthogonality condition between the different mixed-symmetry directions. This yields the expansion coefficients

$$\begin{aligned} \int [d^2 \vec{k}_{\perp, \xi}] [dx_\xi] \psi_{L[4]}^m(x, k_\perp) e^{\pm i \phi_\delta} &= C_{L[4]}^\perp \delta_{m, \mp 1}, \\ \int [d^2 \vec{k}_{\perp, \xi}] [dx_\xi] \psi_{L[4]}^0(x, k_\perp) x_j &= C_{L[4]}^\parallel \delta_{j, \delta}, \\ \int [d^2 \vec{k}_{\perp, \xi}] [dx_\xi] \psi_{L[31]_i}^0(x, k_\perp) x_j &= C_{L[31]}^\parallel \delta_{ij} \quad (\text{C10}) \end{aligned}$$

As we have shown in Sec. IV, the light cone P wave for different representation can be expressed as

$$\begin{aligned} \psi_{L[4]}^{+1}(x, k_\perp) &= (0.394653 + 0.29994i) \psi_2(x, k_\perp) \\ &\quad + (-0.24334 + 0.931223i) \psi_3(x, k_\perp) \\ \psi_{L[4]}^{-1}(x, k_\perp) &= (0.641508 - 0.618858i) \psi_2(x, k_\perp) \\ &\quad - (0.334356 + 0.045252i) \psi_3(x, k_\perp), \\ \psi_{L[31]_\alpha}^0(x, k_\perp) &= \psi_8(x, k_\perp), \\ \psi_{L[31]_\beta}^0(x, k_\perp) &= (0.053i + 0.526) \psi_6(x, k_\perp) \\ &\quad + (-0.580 + 0.620i) \psi_9(x, k_\perp) \\ \psi_{L[31]_\gamma}^0(x, k_\perp) &= (0.475 - 0.372i) \psi_5(x, k_\perp) \\ &\quad + (0.291i - 0.742) \psi_{10}(x, k_\perp) \\ \psi_{L[4]_\delta}^0(x, k_\perp) &= (-0.521 + 0.352i) \psi_4(x, k_\perp) \\ &\quad + (0.725 + 0.280i) \psi_{11}(x, k_\perp) \end{aligned} \quad (\text{C11})$$

The subscript represent L_z component. These wave functions are then coupled to the spin-flavor and color blocks of the OSFC basis and projected onto the fully antisymmetric [1111] irrep of S_4 in the q^4 subsystem. This produces the complete set of light-front P -wave pentaquark basis states with definite (I, S, J^P) used throughout the manuscript and makes explicit that the algebraic OSFC construction and the projection-based implementation differ only by a unitary rotation within degenerate symmetry sectors.

Appendix D: Light-front S -wave three quark orbital states

For the spin orbital interaction, the mixing between S wave three quark state and P wave penta state is generated by the transverse part, the light cone wave function of three quark state can be diagonalized by the full

Hamiltonian,

$$\begin{aligned} H_{LF}^N &\equiv \sum_{i=1}^3 \frac{k_{i\perp}^2 + m_Q^2}{x_i} + 3\sigma_T a_N \\ &- \frac{\sigma_T}{a_N} \sum_{\xi=\alpha, \beta} ((\partial/\partial x_\xi)^2 + M^2(\partial/\partial \vec{k}_{\xi\perp})^2) \quad (\text{D1}) \end{aligned}$$

To diagonalize the Hamiltonian, the longitudinal basis are obtained using Slater determinant with $N = 3$.

$$\varphi_{\bar{n}}[N=3] = \frac{1}{3^{3/4}} \begin{vmatrix} 1 & 1 & 1 \\ e^{i\bar{n}_{21}\bar{s}'_1} & e^{i\bar{n}_{21}\bar{s}'_2} & e^{i\bar{n}_{21}\bar{s}'_3} \\ e^{i\bar{n}_{31}\bar{s}'_1} & e^{i\bar{n}_{31}\bar{s}'_2} & e^{i\bar{n}_{31}\bar{s}'_3} \end{vmatrix} \quad (\text{D2})$$

with

$$\begin{aligned} \bar{s}'_1 &= \frac{1}{6} (\sqrt{2}x_\alpha + \sqrt{6}x_\beta + 2), \\ \bar{s}'_2 &= -\frac{1}{3} (\sqrt{2}x_\alpha), \\ \bar{s}'_3 &= \frac{1}{6} (\sqrt{2}x_\alpha - \sqrt{6}x_\beta - 2), \end{aligned} \quad (\text{D3})$$

The transverse basis for $\xi = \alpha, \beta$ are chosen to be generalized Laguerre polynomials as given in Eq. (C7). Since we are interested in the S wave three quark state, we set $m_\alpha = m_\beta = 0$, and impose the truncation condition $2n_\alpha + 2n_\beta + 2 \leq 10$. By minimizing the ground state mass, we find $a_N = 4.35$. The ground state of light cone Hamiltonian defined in Eq. (D1) corresponds to the wave function $\psi_S(x, k_\perp)$ given in Eq. (60).

Appendix E: Explicit wavefunctions

1. Nucleon OSFC

The bare nucleon state $|N\rangle$ is a three-quark state in the S -wave,

$$|N\rangle = L[3]SF_3[3]C_3[111] \quad (\text{E1})$$

with

$$\begin{aligned} C_3[111] &= \frac{1}{\sqrt{6}} (|RGB\rangle - |RBG\rangle \\ &\quad + |GBR\rangle - |GRB\rangle + |BRG\rangle - |BGR\rangle) \end{aligned} \quad (\text{E2})$$

and

$$\begin{aligned} SF_3[3] &= \frac{1}{\sqrt{2}} (S_3[21]_\alpha F_3[21]_\alpha + S_3[21]_\beta F_3[21]_\beta) = \\ &\frac{1}{\sqrt{18}} [2|u \uparrow u \uparrow d \downarrow\rangle - |u \uparrow u \downarrow d \uparrow\rangle - |u \downarrow u \uparrow d \uparrow\rangle \\ &\quad + 2|u \uparrow d \downarrow u \uparrow\rangle - |u \uparrow d \uparrow u \downarrow\rangle - |u \downarrow d \uparrow u \uparrow\rangle \\ &\quad + 2|d \downarrow u \uparrow u \uparrow\rangle - |d \uparrow u \uparrow u \downarrow\rangle - |d \uparrow u \downarrow u \uparrow\rangle] \end{aligned} \quad (\text{E3})$$

this is the wavefunction of proton and for neutron we just need replace u with d .

2. Pentastates OSFC

For the 4 quarks in the pentaquarkwavefunction the color partition must be $C[211]$ and we choose the Young tableaux and wave function to be

$$C[211]_\alpha = \begin{array}{|c|c|} \hline 1 & 3 \\ \hline 2 & \\ \hline 4 & \\ \hline \end{array} \begin{array}{|c|c|} \hline R & C \\ \hline G & \\ \hline B & \\ \hline \end{array} \quad C[211]_\beta = \begin{array}{|c|c|} \hline 1 & 2 \\ \hline 3 & \\ \hline 4 & \\ \hline \end{array} \begin{array}{|c|c|} \hline R & C \\ \hline G & \\ \hline B & \\ \hline \end{array} \quad [211]_\gamma = \begin{array}{|c|c|} \hline 1 & 4 \\ \hline 2 & \\ \hline 3 & \\ \hline \end{array} \begin{array}{|c|c|} \hline R & C \\ \hline G & \\ \hline B & \\ \hline \end{array} \quad (E4)$$

the $C = R, G, B$ can be three color and the explicit form are

$$C[211]_\alpha(R) = \frac{1}{\sqrt{48}}(3|RGRB\rangle - 3|GRRB\rangle - 3|RBRG\rangle + 3|BRRG\rangle - |RGBR\rangle + |GRBR\rangle + |RBGR\rangle - |BRGR\rangle + 2|GBRR\rangle - 2|BGRR\rangle) \quad (E5a)$$

$$C[211]_\beta(R) = \frac{1}{\sqrt{16}}(2|RRGB\rangle - 2|RRBG\rangle - |RGRB\rangle - |GRRB\rangle + |RBRG\rangle + |BRRG\rangle + |RGBR\rangle + |GRBR\rangle - |RBGR\rangle - |BRGR\rangle) \quad (E5b)$$

$$C[211]_\gamma(R) = \frac{1}{\sqrt{6}}(|BRGR\rangle + |RGBR\rangle + |GBRR\rangle - |RBGR\rangle - |GRBR\rangle - |BGRR\rangle) \quad (E5c)$$

and $C = G, B$ will be

$$C[211]_\alpha(G) = \frac{1}{\sqrt{48}}(3|RGGB\rangle - 3|GRGB\rangle - 3|BGGR\rangle + 3|GBGR\rangle - |RGBG\rangle + |GRBG\rangle - |GBRG\rangle + |BGRG\rangle + 2|BRGG\rangle - 2|RBGG\rangle) \quad (E6a)$$

$$C[211]_\beta(G) = \frac{1}{\sqrt{16}}(2|GGBR\rangle - 2|GGRB\rangle + |RGGB\rangle + |GRGB\rangle - |RGBG\rangle - |GRBG\rangle + |GBRG\rangle + |BGRG\rangle - |GBGR\rangle - |BGGR\rangle) \quad (E6b)$$

$$C[211]_\gamma(G) = \frac{1}{\sqrt{6}}(|RGBG\rangle - |GRBG\rangle - |RBGG\rangle + |BRGG\rangle + |GBRG\rangle - |BGRG\rangle) \quad (E6c)$$

$$C[211]_\alpha(B) = \frac{1}{\sqrt{48}}(3|BRBG\rangle - 3|RBBG\rangle + 3|GBBR\rangle - 3|BGBR\rangle + |RBGB\rangle - |BRGB\rangle - |GBRB\rangle + |BGRB\rangle + 2|RGBB\rangle - 2|GRBB\rangle) \quad (E7a)$$

$$C[211]_\beta(B) = \frac{1}{\sqrt{16}}(2|BBRG\rangle - 2|BBGR\rangle + |RBGB\rangle + |BRGB\rangle - |GBRB\rangle - |BGRB\rangle - |RBBG\rangle - |BRBG\rangle + |GBBR\rangle + |BGBR\rangle) \quad (E7b)$$

$$C[211]_\gamma(B) = \frac{1}{\sqrt{6}}(|RGBB\rangle - |GRBB\rangle - |RBGB\rangle + |BRGB\rangle + |GBRB\rangle - |BGRB\rangle) \quad (E7c)$$

The five quark wave function is

$$C[211]_\xi = \frac{1}{\sqrt{3}}(C[211]_\xi(R)\bar{R} + C[211]_\xi(G)\bar{G} + C[211]_\xi(B)\bar{B}) \quad (E8)$$

where $\bar{C} = \bar{R}, \bar{G}, \bar{B}$ is the antiquark colors. The full OSFC wavefunction is then

$$\Psi = \frac{1}{\sqrt{3}}[C[211]_\beta(LSF[31])_\alpha - C[211]_\alpha(LSF[31])_\beta + C[211]_\gamma(LSF[31])_\gamma] \quad (E9)$$

The $LSF[31]$ wavefunction can be generated by the group decomposition rule(B), the S wave function for five quarks can be generated by recoupling through pertinent Clebsch-Gordon coefficients

$$S[4] \left[\begin{array}{c} 5 \\ 2 \end{array} \right] = |\uparrow\uparrow\uparrow\uparrow\bar{\uparrow}\rangle \quad (E10)$$

and

$$S[4] \left[\begin{smallmatrix} 3 & 3 \\ 2 & 2 \end{smallmatrix} \right] = \sqrt{\frac{4}{5}} (|\uparrow\uparrow\uparrow\downarrow\rangle) - \sqrt{\frac{1}{20}} (|\uparrow\uparrow\uparrow\downarrow\bar{\uparrow}\rangle + |\uparrow\uparrow\downarrow\downarrow\bar{\uparrow}\rangle + |\uparrow\downarrow\uparrow\uparrow\bar{\uparrow}\rangle + |\downarrow\uparrow\uparrow\uparrow\bar{\uparrow}\rangle) \quad (\text{E11})$$

and

$$\begin{aligned} S[22]_{\alpha} \left[\begin{smallmatrix} 1 & 1 \\ 2 & 2 \end{smallmatrix} \right] &= \sqrt{\frac{1}{4}} (|\uparrow\downarrow\uparrow\downarrow\bar{\uparrow}\rangle - |\downarrow\uparrow\uparrow\downarrow\bar{\uparrow}\rangle - |\uparrow\downarrow\uparrow\uparrow\bar{\uparrow}\rangle + |\downarrow\downarrow\uparrow\uparrow\bar{\uparrow}\rangle) \\ S[22]_{\beta} \left[\begin{smallmatrix} 1 & 1 \\ 2 & 2 \end{smallmatrix} \right] &= \sqrt{\frac{1}{12}} (2|\uparrow\uparrow\downarrow\downarrow\bar{\uparrow}\rangle - |\uparrow\downarrow\uparrow\downarrow\bar{\uparrow}\rangle - |\downarrow\uparrow\uparrow\downarrow\bar{\uparrow}\rangle - |\uparrow\downarrow\uparrow\uparrow\bar{\uparrow}\rangle - |\downarrow\downarrow\uparrow\uparrow\bar{\uparrow}\rangle + 2|\downarrow\downarrow\uparrow\uparrow\bar{\uparrow}\rangle) \end{aligned} \quad (\text{E12})$$

and

$$\begin{aligned} S[31]_{\alpha} \left[\begin{smallmatrix} 3 & 3 \\ 2 & 2 \end{smallmatrix} \right] &= \sqrt{\frac{1}{2}} (|\uparrow\downarrow\uparrow\uparrow\bar{\uparrow}\rangle - |\downarrow\uparrow\uparrow\uparrow\bar{\uparrow}\rangle) \\ S[31]_{\beta} \left[\begin{smallmatrix} 3 & 3 \\ 2 & 2 \end{smallmatrix} \right] &= \sqrt{\frac{1}{6}} (2|\uparrow\uparrow\downarrow\uparrow\bar{\uparrow}\rangle - |\uparrow\downarrow\uparrow\uparrow\bar{\uparrow}\rangle - |\downarrow\uparrow\uparrow\uparrow\bar{\uparrow}\rangle) \\ S[31]_{\gamma} \left[\begin{smallmatrix} 3 & 3 \\ 2 & 2 \end{smallmatrix} \right] &= \sqrt{\frac{1}{12}} (3|\uparrow\uparrow\uparrow\downarrow\bar{\uparrow}\rangle - |\uparrow\uparrow\downarrow\uparrow\bar{\uparrow}\rangle - |\uparrow\downarrow\uparrow\uparrow\bar{\uparrow}\rangle - |\downarrow\uparrow\uparrow\uparrow\bar{\uparrow}\rangle) \end{aligned} \quad (\text{E13})$$

and

$$\begin{aligned} S[31]_{\alpha} \left[\begin{smallmatrix} 1 & 1 \\ 2 & 2 \end{smallmatrix} \right] &= \sqrt{\frac{1}{3}} (|\uparrow\downarrow\uparrow\uparrow\bar{\downarrow}\rangle - |\downarrow\uparrow\uparrow\uparrow\bar{\downarrow}\rangle) - \sqrt{\frac{1}{12}} (|\uparrow\downarrow\uparrow\downarrow\bar{\uparrow}\rangle + |\uparrow\downarrow\uparrow\uparrow\bar{\uparrow}\rangle - |\downarrow\uparrow\uparrow\downarrow\bar{\uparrow}\rangle - |\downarrow\uparrow\uparrow\uparrow\bar{\uparrow}\rangle) \\ S[31]_{\beta} \left[\begin{smallmatrix} 1 & 1 \\ 2 & 2 \end{smallmatrix} \right] &= \frac{1}{3} (2|\uparrow\uparrow\downarrow\uparrow\bar{\downarrow}\rangle - |\uparrow\downarrow\uparrow\uparrow\bar{\downarrow}\rangle - |\downarrow\uparrow\uparrow\uparrow\bar{\downarrow}\rangle) \\ &\quad - \frac{1}{6} (2|\uparrow\uparrow\downarrow\downarrow\bar{\uparrow}\rangle - |\uparrow\downarrow\uparrow\downarrow\bar{\uparrow}\rangle - |\downarrow\uparrow\uparrow\downarrow\bar{\uparrow}\rangle + |\uparrow\downarrow\uparrow\uparrow\bar{\uparrow}\rangle + |\downarrow\downarrow\uparrow\uparrow\bar{\uparrow}\rangle - 2|\downarrow\downarrow\uparrow\uparrow\bar{\uparrow}\rangle) \\ S[31]_{\gamma} \left[\begin{smallmatrix} 1 & 1 \\ 2 & 2 \end{smallmatrix} \right] &= \sqrt{\frac{1}{18}} (3|\uparrow\downarrow\uparrow\uparrow\bar{\downarrow}\rangle - |\downarrow\uparrow\uparrow\uparrow\bar{\downarrow}\rangle - |\uparrow\uparrow\downarrow\uparrow\bar{\downarrow}\rangle - |\uparrow\uparrow\uparrow\downarrow\bar{\downarrow}\rangle) \\ &\quad - \sqrt{\frac{1}{18}} (|\uparrow\uparrow\downarrow\downarrow\bar{\uparrow}\rangle + |\uparrow\downarrow\uparrow\downarrow\bar{\uparrow}\rangle + |\downarrow\uparrow\uparrow\downarrow\bar{\uparrow}\rangle - |\uparrow\downarrow\uparrow\uparrow\bar{\uparrow}\rangle - |\downarrow\downarrow\uparrow\uparrow\bar{\uparrow}\rangle - |\downarrow\downarrow\uparrow\uparrow\bar{\uparrow}\rangle) \end{aligned} \quad (\text{E14})$$

Note that the anti-quark spin satisfies $\bar{\uparrow} = -i\sigma^2 \uparrow = \downarrow$ and $\bar{\downarrow} = -i\sigma^2 \downarrow = \uparrow$, and the flavor function follow the similar rules, we just need to replace the $\uparrow \rightarrow u, \downarrow \rightarrow d$ and $\bar{\uparrow} \rightarrow \bar{d}, \bar{\downarrow} \rightarrow \bar{u}$, the isospin of antiquark is $I_z(\bar{u}) = -\frac{1}{2}, I_z(\bar{d}) = +\frac{1}{2}$ for example, the full pentaquark wavefunction for isospin 1/2 and spin 5/2 can be written as

$$\begin{aligned} \varphi_{S[4]F[31]}^{L[4]SF[31]} \left[\begin{smallmatrix} 1 & 1 \\ 2 & 2 \end{smallmatrix}, \begin{smallmatrix} 5 & 5 \\ 2 & 2 \end{smallmatrix} \right] &= \frac{1}{\sqrt{3}} L[4] S[4] (C[211]_{\beta} F[31]_{\alpha} - C[211]_{\alpha} F[31]_{\beta} + C[211]_{\gamma} F[31]_{\gamma}) \\ &= \frac{1}{\sqrt{3}} L[4] |\uparrow\uparrow\uparrow\uparrow\bar{\uparrow}\rangle \left(C[211]_{\beta} \left(\sqrt{\frac{1}{3}} (|uduu\bar{u}\rangle - |duuu\bar{u}\rangle) - \sqrt{\frac{1}{12}} (|ududd\bar{d}\rangle + |uddud\bar{d}\rangle - |duudd\bar{d}\rangle - |dudud\bar{d}\rangle) \right) \right. \\ &\quad - C[211]_{\alpha} \left(\frac{1}{3} (2|uudu\bar{u}\rangle - |uduu\bar{u}\rangle - |duuu\bar{u}\rangle) - \frac{1}{6} (2|uudd\bar{d}\rangle - |ududd\bar{d}\rangle - |duudd\bar{d}\rangle + |uddud\bar{d}\rangle) \right. \\ &\quad \left. \left. + |dudud\bar{d}\rangle - 2|dduud\bar{d}\rangle \right) + C[211]_{\gamma} \left(\sqrt{\frac{1}{18}} (3|uduu\bar{u}\rangle - |duuu\bar{u}\rangle - |uudu\bar{u}\rangle - |uuud\bar{u}\rangle) \right. \right. \\ &\quad \left. \left. - \sqrt{\frac{1}{18}} (|uudd\bar{d}\rangle + |uddud\bar{d}\rangle + |duudd\bar{d}\rangle - |uddud\bar{d}\rangle - |dudud\bar{d}\rangle - |dduud\bar{d}\rangle) \right) \right) \\ \varphi_{S[4]F[31]}^{L[31]SF[31]} \left[\begin{smallmatrix} 1 & 1 \\ 2 & 2 \end{smallmatrix}, \begin{smallmatrix} 5 & 5 \\ 2 & 2 \end{smallmatrix} \right] &= \frac{1}{\sqrt{3}} S[4] \left(C[211]_{\beta} \left[\frac{1}{\sqrt{3}} (L_5[31]_{\alpha} F[31]_{\beta} + \alpha \leftrightarrow \beta) + \frac{1}{\sqrt{6}} (L[31]_{\alpha} F[31]_{\gamma} + \alpha \leftrightarrow \gamma) \right] \right. \\ &\quad - C[211]_{\alpha} \left[\frac{1}{\sqrt{3}} (L[31]_{\alpha} F[31]_{\alpha} - \alpha \rightarrow \beta) + \frac{1}{\sqrt{6}} (L[31]_{\gamma} F[31]_{\beta} + \gamma \leftrightarrow \beta) \right] \\ &\quad \left. + C[211]_{\gamma} \left[\frac{1}{\sqrt{6}} (L[31]_{\alpha} F[31]_{\alpha} + \alpha \rightarrow \beta) - \frac{2}{\sqrt{6}} L[31]_{\gamma} F[31]_{\gamma} \right] \right) \end{aligned} \quad (\text{E15})$$

$$\begin{aligned}
\varphi_{S[4]F[22]}^{L[31]SF[22]} \left[\frac{1}{2} \frac{1}{2}, \frac{5}{2} \frac{5}{2} \right] &= \frac{1}{\sqrt{3}} S[4] \left(C[211]_{\beta} \left[\frac{1}{2} (F[22]_{\alpha} L[31]_{\beta} + \alpha \leftrightarrow \beta) - \frac{1}{\sqrt{2}} F[22]_{\alpha} L[31]_{\gamma} \right] \right. \\
&\quad - C[211]_{\alpha} \left[\frac{1}{2} (F[22]_{\alpha} L[31]_{\alpha} - \alpha \rightarrow \beta) - \frac{1}{\sqrt{2}} F[22]_{\beta} L[31]_{\gamma} \right] \\
&\quad \left. - C[211]_{\gamma} \left[\frac{1}{\sqrt{2}} (F[22]_{\alpha} L[31]_{\alpha} + \alpha \rightarrow \beta) \right] \right) \tag{E16}
\end{aligned}$$

We only show the maximum weight representations, the state with lower S_z component can be obtained by applying the spin lowering operator. The wavefunction for isospin 1/2 and spin 3/2 can be written as

$$\begin{aligned}
\varphi_{S[31]F[31]}^{L[4]SF[31]_a} \left[\frac{1}{2} \frac{1}{2}, \frac{3}{2} \frac{3}{2} \right] &= \frac{1}{\sqrt{3}} L[4] \left(C[211]_{\beta} \left[\frac{1}{\sqrt{3}} (S[31]_{\alpha} F[31]_{\beta} + \alpha \leftrightarrow \beta) + \frac{1}{\sqrt{6}} (S[31]_{\alpha} F[31]_{\gamma} + \alpha \leftrightarrow \gamma) \right] \right. \\
&\quad - C[211]_{\alpha} \left[\frac{1}{\sqrt{3}} (S[31]_{\alpha} F[31]_{\alpha} - \alpha \rightarrow \beta) + \frac{1}{\sqrt{6}} (S[31]_{\gamma} F[31]_{\beta} + \gamma \leftrightarrow \beta) \right] \\
&\quad \left. + C[211]_{\gamma} \left[\frac{1}{\sqrt{6}} (S[31]_{\alpha} F[31]_{\alpha} + \alpha \rightarrow \beta) - \frac{2}{\sqrt{6}} S[31]_{\gamma} F[31]_{\gamma} \right] \right) \tag{E17}
\end{aligned}$$

$$\begin{aligned}
\varphi_{S[31]F[22]}^{L[4]SF[31]_b} \left[\frac{1}{2} \frac{1}{2}, \frac{3}{2} \frac{3}{2} \right] &= \frac{1}{\sqrt{3}} L[4] \left(C[211]_{\beta} \left[\frac{1}{2} (F[22]_{\alpha} S[31]_{\beta} + \alpha \leftrightarrow \beta) - \frac{1}{\sqrt{2}} F[22]_{\alpha} S[31]_{\gamma} \right] \right. \\
&\quad - C[211]_{\alpha} \left[\frac{1}{2} (F[22]_{\alpha} S[31]_{\alpha} - \alpha \rightarrow \beta) - \frac{1}{\sqrt{2}} F[22]_{\beta} S[31]_{\gamma} \right] \\
&\quad \left. - C[211]_{\gamma} \left[\frac{1}{\sqrt{2}} (F[22]_{\alpha} S[31]_{\alpha} + \alpha \rightarrow \beta) \right] \right) \tag{E18}
\end{aligned}$$

$$\varphi_{S[4]F[31]}^{L[4]SF[31]_c} \left[\frac{1}{2} \frac{1}{2}, \frac{3}{2} \frac{3}{2} \right] = \frac{1}{\sqrt{3}} L[4] S[4] (C[211]_{\beta} F[31]_{\alpha} - C[211]_{\alpha} F[31]_{\beta} + C[211]_{\gamma} F[31]_{\gamma}) \tag{E19}$$

$$\begin{aligned}
\varphi_{S[31]F[31]}^{L[31]SF[31]_a} \left[\frac{1}{2} \frac{1}{2}, \frac{3}{2} \frac{3}{2} \right] &= \frac{1}{\sqrt{3}} \left(C[211]_{\beta} \left[\frac{1}{\sqrt{3}} (L[31]_{\alpha} SF[31]_{\beta} + \alpha \leftrightarrow \beta) + \frac{1}{\sqrt{6}} (L[31]_{\alpha} SF[31]_{\gamma} + \alpha \leftrightarrow \gamma) \right] \right. \\
&\quad - C[211]_{\alpha} \left[\frac{1}{\sqrt{3}} (L[31]_{\alpha} SF[31]_{\alpha} - \alpha \rightarrow \beta) + \frac{1}{\sqrt{6}} (L[31]_{\gamma} SF[31]_{\beta} + \gamma \leftrightarrow \beta) \right] \\
&\quad \left. + C[211]_{\gamma} \left[\frac{1}{\sqrt{6}} (L[31]_{\alpha} SF[31]_{\alpha} + \alpha \rightarrow \beta) - \frac{2}{\sqrt{6}} L[31]_{\gamma} SF[31]_{\gamma} \right] \right) \tag{E20}
\end{aligned}$$

$$\begin{cases} SF[31]_{\alpha} = \left[\frac{1}{\sqrt{3}} (S[31]_{\alpha} F[31]_{\beta} + \alpha \leftrightarrow \beta) + \frac{1}{\sqrt{6}} (S[31]_{\alpha} F[31]_{\gamma} + \alpha \leftrightarrow \gamma) \right] \\ SF[31]_{\beta} = \left[\frac{1}{\sqrt{3}} (S[31]_{\alpha} F[31]_{\alpha} - \alpha \rightarrow \beta) + \frac{1}{\sqrt{6}} (S[31]_{\gamma} F[31]_{\beta} + \gamma \leftrightarrow \beta) \right] \\ SF[31]_{\gamma} = \left[\frac{1}{\sqrt{6}} (S[31]_{\alpha} F[31]_{\alpha} + \alpha \rightarrow \beta) - \frac{2}{\sqrt{6}} S[31]_{\gamma} F[31]_{\gamma} \right] \end{cases}$$

$$\begin{aligned}
\varphi_{S[31]F[22]}^{L[31]SF[31]_b} \left[\frac{1}{2} \frac{1}{2}, \frac{3}{2} \frac{3}{2} \right] &= \frac{1}{\sqrt{3}} \left(C[211]_{\beta} \left[\frac{1}{\sqrt{3}} (L[31]_{\alpha} SF[31]_{\beta} + \alpha \leftrightarrow \beta) + \frac{1}{\sqrt{6}} (L[31]_{\alpha} SF[31]_{\gamma} + \alpha \leftrightarrow \gamma) \right] \right. \\
&\quad - C[211]_{\alpha} \left[\frac{1}{\sqrt{3}} (L[31]_{\alpha} SF[31]_{\alpha} - \alpha \rightarrow \beta) + \frac{1}{\sqrt{6}} (L[31]_{\gamma} SF[31]_{\beta} + \gamma \leftrightarrow \beta) \right] \\
&\quad \left. + C[211]_{\gamma} \left[\frac{1}{\sqrt{6}} (L[31]_{\alpha} SF[31]_{\alpha} + \alpha \rightarrow \beta) - \frac{2}{\sqrt{6}} L[31]_{\gamma} SF[31]_{\gamma} \right] \right) \tag{E21}
\end{aligned}$$

$$\begin{cases} SF[31]_{\alpha} = \left[\frac{1}{2} (F[22]_{\alpha} S[31]_{\beta} + \alpha \leftrightarrow \beta) - \frac{1}{\sqrt{2}} F[22]_{\alpha} S[31]_{\gamma} \right] \\ SF[31]_{\beta} = \left[\frac{1}{2} (F[22]_{\alpha} S[31]_{\alpha} - \alpha \rightarrow \beta) - \frac{1}{\sqrt{2}} F[22]_{\beta} S[31]_{\gamma} \right] \\ SF[31]_{\gamma} = - \left[\frac{1}{\sqrt{2}} (F[22]_{\alpha} S[31]_{\alpha} + \alpha \rightarrow \beta) \right] \end{cases}$$

$$\begin{aligned}
\varphi_{S[4]F[31]}^{L[31]SF[31]_c} \left[\frac{1}{2} \frac{1}{2}, \frac{3}{2} \frac{3}{2} \right] &= \frac{1}{\sqrt{3}} S[4] \left(C[211]_{\beta} \left[\frac{1}{\sqrt{3}} (L[31]_{\alpha} F[31]_{\beta} + \alpha \leftrightarrow \beta) + \frac{1}{\sqrt{6}} (L[31]_{\alpha} F[31]_{\gamma} + \alpha \leftrightarrow \gamma) \right] \right. \\
&\quad \left. - C[211]_{\alpha} \left[\frac{1}{\sqrt{3}} (L[31]_{\alpha} F[31]_{\alpha} - \alpha \rightarrow \beta) + \frac{1}{\sqrt{6}} (L[31]_{\gamma} F[31]_{\beta} + \gamma \leftrightarrow \beta) \right] \right)
\end{aligned}$$

$$+C[211]_\gamma \left[\frac{1}{\sqrt{6}} (L[31]_\alpha F[31]_\alpha + \alpha \rightarrow \beta) - \frac{2}{\sqrt{6}} L[31]_\gamma F[31]_\gamma \right) \right] \quad (\text{E22})$$

$$\begin{aligned} \varphi_{S[31]F[31]}^{L[31]SF[22]_\alpha} \left[\frac{1}{2} \frac{1}{2}, \frac{3}{2} \frac{3}{2} \right] &= \frac{1}{\sqrt{3}} \left(C[211]_\beta \left[\frac{1}{2} (SF[22]_\alpha L[31]_\beta + \alpha \leftrightarrow \beta) - \frac{1}{\sqrt{2}} SF[22]_\alpha L[31]_\gamma \right] \right. \\ &\quad - C[211]_\alpha \left[\frac{1}{2} (SF[22]_\alpha L[31]_\alpha - \alpha \rightarrow \beta) - \frac{1}{\sqrt{2}} SF[22]_\beta L[31]_\gamma \right] \\ &\quad \left. - C[211]_\gamma \left[\frac{1}{\sqrt{2}} (SF[22]_\alpha L[31]_\alpha + \alpha \rightarrow \beta) \right] \right) \end{aligned} \quad (\text{E23})$$

$$\begin{aligned} &\begin{cases} SF[22]_\alpha = \left[\frac{1}{\sqrt{6}} (S[31]_\alpha F[31]_\beta + \alpha \leftrightarrow \beta) - \frac{1}{\sqrt{3}} (S[31]_\alpha F[31]_\gamma + \alpha \leftrightarrow \gamma) \right] \\ SF[22]_\beta = \left[\frac{1}{\sqrt{6}} (S[31]_\alpha F[31]_\alpha - \alpha \leftrightarrow \beta) - \frac{1}{\sqrt{3}} (S[31]_\beta F[31]_\gamma + \beta \leftrightarrow \gamma) \right] \end{cases} \\ \varphi_{S[4]F[22]}^{L[31]SF[22]_b} \left[\frac{1}{2} \frac{1}{2}, \frac{3}{2} \frac{3}{2} \right] &= \frac{1}{\sqrt{3}} S[4] \left(C[211]_\beta \left[\frac{1}{2} (F[22]_\alpha L[31]_\beta + \alpha \leftrightarrow \beta) - \frac{1}{\sqrt{2}} F[22]_\alpha L[31]_\gamma \right] \right. \\ &\quad - C[211]_\alpha \left[\frac{1}{2} (F[22]_\alpha L[31]_\alpha - \alpha \rightarrow \beta) - \frac{1}{\sqrt{2}} F[22]_\beta L[31]_\gamma \right] \\ &\quad \left. - C[211]_\gamma \left[\frac{1}{\sqrt{2}} (F[22]_\alpha L[31]_\alpha + \alpha \rightarrow \beta) \right] \right) \\ \varphi_{S[31]F[31]}^{L[31]SF[4]} \left[\frac{1}{2} \frac{1}{2}, \frac{3}{2} \frac{3}{2} \right] &= \frac{1}{3} (C[211]_\beta L[31]_\alpha - C[211]_\alpha L[31]_\beta + C[211]_\gamma L[31]_\gamma) \\ &\quad (S[31]_\alpha F[31]_\alpha + S[31]_\beta F[31]_\beta + S[31]_\gamma F[31]_\gamma) \end{aligned} \quad (\text{E24})$$

$$\begin{aligned} \varphi_{S[31]F[31]}^{L[31]SF[211]_\alpha} \left[\frac{1}{2} \frac{1}{2}, \frac{3}{2} \frac{3}{2} \right] &= \frac{1}{\sqrt{3}} \left(C[211]_\beta \frac{1}{\sqrt{2}} [L[31]_\gamma SF[211]_\alpha + L[31]_\beta SF[211]_\gamma] \right. \\ &\quad - C[211]_\alpha \frac{1}{\sqrt{2}} [L[31]_\gamma SF[211]_\beta - L[31]_\alpha SF[211]_\gamma] \\ &\quad \left. - C[211]_\gamma \frac{1}{\sqrt{2}} [L[31]_\alpha SF[211]_\alpha + L[31]_\beta SF[211]_\beta] \right) \end{aligned} \quad (\text{E25})$$

$$\begin{aligned} &\begin{cases} SF[211]_\alpha = \frac{1}{\sqrt{2}} [S[31]_\alpha F[31]_\gamma - S[31]_\gamma F[31]_\alpha] \\ SF[211]_\beta = \frac{1}{\sqrt{2}} [S[31]_\beta F[31]_\gamma - S[31]_\gamma F[31]_\beta] \\ SF[211]_\gamma = \frac{1}{\sqrt{2}} [S[31]_\alpha F[31]_\beta - S[31]_\beta F[31]_\alpha] \end{cases} \\ \varphi_{S[31]F[22]}^{L[31]SF[211]_b} \left[\frac{1}{2} \frac{1}{2}, \frac{3}{2} \frac{3}{2} \right] &= \frac{1}{\sqrt{3}} \left(C[211]_\beta \frac{1}{\sqrt{2}} [L[31]_\gamma SF[211]_\alpha + L[31]_\beta SF[211]_\gamma] \right. \\ &\quad - C[211]_\alpha \frac{1}{\sqrt{2}} [L[31]_\gamma SF[211]_\beta - L[31]_\alpha SF[211]_\gamma] \\ &\quad \left. - C[211]_\gamma \frac{1}{\sqrt{2}} [L[31]_\alpha SF[211]_\alpha + L[31]_\beta SF[211]_\beta] \right) \\ &\begin{cases} SF[211]_\alpha = \frac{1}{2} [S[31]_\alpha F[22]_\beta + S[31]_\beta F[22]_\alpha + \sqrt{2} S[31]_\gamma F[22]_\alpha] \\ SF[211]_\beta = \frac{1}{2} [S[31]_\alpha F[22]_\alpha - S[31]_\beta F[22]_\beta + \sqrt{2} S[31]_\gamma F[22]_\beta] \\ SF[211]_\gamma = \frac{1}{\sqrt{2}} [S[31]_\alpha F[22]_\beta - S[31]_\beta F[22]_\alpha] \end{cases} \end{aligned} \quad (\text{E26})$$

The wavefunction for isospin 1/2 and spin 1/2 can be written as

$$\begin{aligned} \varphi_{S[31]F[31]}^{L[4]SF[31]_\alpha} \left[\frac{1}{2} \frac{1}{2}, \frac{1}{2} \frac{1}{2} \right] &= \frac{1}{\sqrt{3}} L[4] \left(C[211]_\beta \left[\frac{1}{\sqrt{3}} (S[31]_\alpha F[31]_\beta + \alpha \leftrightarrow \beta) + \frac{1}{\sqrt{6}} (S[31]_\alpha F[31]_\gamma + \alpha \leftrightarrow \gamma) \right] \right. \\ &\quad \left. - C[211]_\alpha \left[\frac{1}{\sqrt{3}} (S[31]_\alpha F[31]_\alpha - \alpha \rightarrow \beta) + \frac{1}{\sqrt{6}} (S[31]_\gamma F[31]_\beta + \gamma \leftrightarrow \beta) \right] \right) \end{aligned}$$

$$+C[211]_\gamma \left[\frac{1}{\sqrt{6}} (S[31]_\alpha F[31]_\alpha + \alpha \rightarrow \beta) - \frac{2}{\sqrt{6}} S[31]_\gamma F[31]_\gamma \right] \quad (\text{E27})$$

$$\begin{aligned} \varphi_{S[31]F[22]}^{L[4]SF[31]b} \left[\frac{1}{2} \frac{1}{2}, \frac{1}{2} \frac{1}{2} \right] &= \frac{1}{\sqrt{3}} L[4] \left(C[211]_\beta \left[\frac{1}{2} (F[22]_\alpha S[31]_\beta + \alpha \leftrightarrow \beta) - \frac{1}{\sqrt{2}} F[22]_\alpha S[31]_\gamma \right] \right. \\ &\quad - C[211]_\alpha \left[\frac{1}{2} (F[22]_\alpha S[31]_\alpha - \alpha \rightarrow \beta) - \frac{1}{\sqrt{2}} F[22]_\beta S[31]_\gamma \right] \\ &\quad \left. - C[211]_\gamma \left[\frac{1}{\sqrt{2}} (F[22]_\alpha S[31]_\alpha + \alpha \rightarrow \beta) \right] \right) \end{aligned} \quad (\text{E28})$$

$$\begin{aligned} \varphi_{S[22]F[31]}^{L[4]SF[31]c} \left[\frac{1}{2} \frac{1}{2}, \frac{1}{2} \frac{1}{2} \right] &= \frac{1}{\sqrt{3}} L[4] \left(C[211]_\beta \left[\frac{1}{2} (S[22]_\alpha F[31]_\beta + \alpha \leftrightarrow \beta) - \frac{1}{\sqrt{2}} S[22]_\alpha F[31]_\gamma \right] \right. \\ &\quad - C[211]_\alpha \left[\frac{1}{2} (S[22]_\alpha F[31]_\alpha - \alpha \rightarrow \beta) - \frac{1}{\sqrt{2}} S[22]_\beta F[31]_\gamma \right] \\ &\quad \left. - C[211]_\gamma \left[\frac{1}{\sqrt{2}} (S[22]_\alpha F[31]_\alpha + \alpha \rightarrow \beta) \right] \right) \end{aligned} \quad (\text{E29})$$

$$\begin{aligned} \varphi_{S[31]F[31]}^{L[31]SF[31]a} \left[\frac{1}{2} \frac{1}{2}, \frac{1}{2} \frac{1}{2} \right] &= \frac{1}{\sqrt{3}} \left(C[211]_\beta \left[\frac{1}{\sqrt{3}} (L[31]_\alpha SF[31]_\beta + \alpha \leftrightarrow \beta) + \frac{1}{\sqrt{6}} (L[31]_\alpha SF[31]_\gamma + \alpha \leftrightarrow \gamma) \right] \right. \\ &\quad - C[211]_\alpha \left[\frac{1}{\sqrt{3}} (L[31]_\alpha SF[31]_\alpha - \alpha \rightarrow \beta) + \frac{1}{\sqrt{6}} (L[31]_\gamma SF[31]_\beta + \gamma \leftrightarrow \beta) \right] \\ &\quad \left. + C[211]_\gamma \left[\frac{1}{\sqrt{6}} (L[31]_\alpha SF[31]_\alpha + \alpha \rightarrow \beta) - \frac{2}{\sqrt{6}} L[31]_\gamma SF[31]_\gamma \right] \right) \end{aligned} \quad (\text{E30})$$

$$\begin{cases} SF[31]_\alpha = \left[\frac{1}{\sqrt{3}} (S[31]_\alpha F[31]_\beta + \alpha \leftrightarrow \beta) + \frac{1}{\sqrt{6}} (S[31]_\alpha F[31]_\gamma + \alpha \leftrightarrow \gamma) \right] \\ SF[31]_\beta = \left[\frac{1}{\sqrt{3}} (S[31]_\alpha F[31]_\alpha - \alpha \rightarrow \beta) + \frac{1}{\sqrt{6}} (S[31]_\gamma F[31]_\beta + \gamma \leftrightarrow \beta) \right] \\ SF[31]_\gamma = \left[\frac{1}{\sqrt{6}} (S[31]_\alpha F[31]_\alpha + \alpha \rightarrow \beta) - \frac{2}{\sqrt{6}} S[31]_\gamma F[31]_\gamma \right] \end{cases}$$

$$\begin{aligned} \varphi_{S[31]F[22]}^{L[31]SF[31]b} \left[\frac{1}{2} \frac{1}{2}, \frac{1}{2} \frac{1}{2} \right] &= \frac{1}{\sqrt{3}} \left(C[211]_\beta \left[\frac{1}{\sqrt{3}} (L[31]_\alpha SF[31]_\beta + \alpha \leftrightarrow \beta) + \frac{1}{\sqrt{6}} (L[31]_\alpha SF[31]_\gamma + \alpha \leftrightarrow \gamma) \right] \right. \\ &\quad - C[211]_\alpha \left[\frac{1}{\sqrt{3}} (L[31]_\alpha SF[31]_\alpha - \alpha \rightarrow \beta) + \frac{1}{\sqrt{6}} (L[31]_\gamma SF[31]_\beta + \gamma \leftrightarrow \beta) \right] \\ &\quad \left. + C[211]_\gamma \left[\frac{1}{\sqrt{6}} (L[31]_\alpha SF[31]_\alpha + \alpha \rightarrow \beta) - \frac{2}{\sqrt{6}} L[31]_\gamma SF[31]_\gamma \right] \right) \end{aligned} \quad (\text{E31})$$

$$\begin{cases} SF[31]_\alpha = \left[\frac{1}{2} (F[22]_\alpha S[31]_\beta + \alpha \leftrightarrow \beta) - \frac{1}{\sqrt{2}} F[22]_\alpha S[31]_\gamma \right] \\ SF[31]_\beta = \left[\frac{1}{2} (F[22]_\alpha S[31]_\alpha - \alpha \rightarrow \beta) - \frac{1}{\sqrt{2}} F[22]_\beta S[31]_\gamma \right] \\ SF[31]_\gamma = - \left[\frac{1}{\sqrt{2}} (F[22]_\alpha S[31]_\alpha + \alpha \rightarrow \beta) \right] \end{cases}$$

$$\begin{aligned} \varphi_{S[22]F[31]}^{L[31]SF[31]c} \left[\frac{1}{2} \frac{1}{2}, \frac{1}{2} \frac{1}{2} \right] &= \frac{1}{\sqrt{3}} \left(C[211]_\beta \left[\frac{1}{\sqrt{3}} (L[31]_\alpha SF[31]_\beta + \alpha \leftrightarrow \beta) + \frac{1}{\sqrt{6}} (L[31]_\alpha SF[31]_\gamma + \alpha \leftrightarrow \gamma) \right] \right. \\ &\quad - C[211]_\alpha \left[\frac{1}{\sqrt{3}} (L[31]_\alpha SF[31]_\alpha - \alpha \rightarrow \beta) + \frac{1}{\sqrt{6}} (L[31]_\gamma SF[31]_\beta + \gamma \leftrightarrow \beta) \right] \\ &\quad \left. + C[211]_\gamma \left[\frac{1}{\sqrt{6}} (L[31]_\alpha SF[31]_\alpha + \alpha \rightarrow \beta) - \frac{2}{\sqrt{6}} L[31]_\gamma SF[31]_\gamma \right] \right) \end{aligned} \quad (\text{E32})$$

$$\begin{cases} SF[31]_\alpha = \left[\frac{1}{2} (S[22]_\alpha F[31]_\beta + \alpha \leftrightarrow \beta) - \frac{1}{\sqrt{2}} S[22]_\alpha F[31]_\gamma \right] \\ SF[31]_\beta = \left[\frac{1}{2} (S[22]_\alpha F[31]_\alpha - \alpha \rightarrow \beta) - \frac{1}{\sqrt{2}} S[22]_\beta F[31]_\gamma \right] \\ SF[31]_\gamma = - \left[\frac{1}{\sqrt{2}} (S[22]_\alpha F[31]_\alpha + \alpha \rightarrow \beta) \right] \end{cases}$$

$$\begin{aligned}
\varphi_{S[31]F[31]}^{L[31]SF[22]a} \left[\frac{1}{2} \frac{1}{2}, \frac{1}{2} \frac{1}{2} \right] &= \frac{1}{\sqrt{3}} \left(C[211]_{\beta} \left[\frac{1}{2} (SF[22]_{\alpha} L[31]_{\beta} + \alpha \leftrightarrow \beta) - \frac{1}{\sqrt{2}} SF[22]_{\alpha} L[31]_{\gamma} \right] \right. \\
&\quad - C[211]_{\alpha} \left[\frac{1}{2} (SF[22]_{\alpha} L[31]_{\alpha} - \alpha \rightarrow \beta) - \frac{1}{\sqrt{2}} SF[22]_{\beta} L[31]_{\gamma} \right] \\
&\quad \left. - C[211]_{\gamma} \left[\frac{1}{\sqrt{2}} (SF[22]_{\alpha} L[31]_{\alpha} + \alpha \rightarrow \beta) \right] \right) \tag{E33}
\end{aligned}$$

$$\begin{cases} SF[22]_{\alpha} = \left[\frac{1}{\sqrt{6}} (S[31]_{\alpha} F[31]_{\beta} + \alpha \leftrightarrow \beta) - \frac{1}{\sqrt{3}} (S[31]_{\alpha} F[31]_{\gamma} + \alpha \leftrightarrow \gamma) \right] \\ SF[22]_{\beta} = \left[\frac{1}{\sqrt{6}} (S[31]_{\alpha} F[31]_{\alpha} - \alpha \leftrightarrow \beta) - \frac{1}{\sqrt{3}} (S[31]_{\beta} F[31]_{\gamma} + \beta \leftrightarrow \gamma) \right] \end{cases}$$

$$\begin{aligned}
\varphi_{S[22]F[22]}^{L[31]SF[22]b} \left[\frac{1}{2} \frac{1}{2}, \frac{1}{2} \frac{1}{2} \right] &= \frac{1}{\sqrt{3}} \left(C[211]_{\beta} \left[\frac{1}{2} (SF[22]_{\alpha} L[31]_{\beta} + \alpha \leftrightarrow \beta) - \frac{1}{\sqrt{2}} SF[22]_{\alpha} L[31]_{\gamma} \right] \right. \\
&\quad - C[211]_{\alpha} \left[\frac{1}{2} (SF[22]_{\alpha} L[31]_{\alpha} - \alpha \rightarrow \beta) - \frac{1}{\sqrt{2}} SF[22]_{\beta} L[31]_{\gamma} \right] \\
&\quad \left. - C[211]_{\gamma} \left[\frac{1}{\sqrt{2}} (SF[22]_{\alpha} L[31]_{\alpha} + \alpha \rightarrow \beta) \right] \right) \tag{E34}
\end{aligned}$$

$$\begin{cases} SF[22]_{\alpha} = \frac{1}{\sqrt{2}} [S[22]_{\alpha} F[22]_{\beta} + \alpha \leftrightarrow \beta] \\ SF[22]_{\beta} = \frac{1}{\sqrt{2}} [S[22]_{\alpha} F[22]_{\alpha} - \alpha \leftrightarrow \beta] \end{cases}$$

$$\begin{aligned}
\varphi_{S[31]F[31]}^{L[31]SF[4]a} \left[\frac{1}{2} \frac{1}{2}, \frac{1}{2} \frac{1}{2} \right] &= \frac{1}{3} (C[211]_{\beta} L[31]_{\alpha} - C[211]_{\alpha} L[31]_{\beta} + C[211]_{\gamma} L[31]_{\gamma}) \\
&\quad (S[31]_{\alpha} F[31]_{\alpha} + S[31]_{\beta} F[31]_{\beta} + S[31]_{\gamma} F[31]_{\gamma}) \tag{E35}
\end{aligned}$$

$$\begin{aligned}
\varphi_{S[22]F[22]}^{L[31]SF[4]b} \left[\frac{1}{2} \frac{1}{2}, \frac{1}{2} \frac{1}{2} \right] &= \frac{1}{\sqrt{6}} (C[211]_{\beta} L[31]_{\alpha} - C[211]_{\alpha} L[31]_{\beta} + C[211]_{\gamma} L[31]_{\gamma}) \\
&\quad (S[22]_{\alpha} F[22]_{\alpha} + S[22]_{\beta} F[22]_{\beta}) \tag{E36}
\end{aligned}$$

$$\begin{aligned}
\varphi_{S[31]F[31]}^{L[31]SF[211]a} \left[\frac{1}{2} \frac{1}{2}, \frac{1}{2} \frac{1}{2} \right] &= \frac{1}{\sqrt{3}} \left(C[211]_{\beta} \frac{1}{\sqrt{2}} [L[31]_{\gamma} SF[211]_{\alpha} + L[31]_{\beta} SF[211]_{\gamma}] \right. \\
&\quad - C[211]_{\alpha} \frac{1}{\sqrt{2}} [L[31]_{\gamma} SF[211]_{\beta} - L[31]_{\alpha} SF[211]_{\gamma}] \\
&\quad \left. - C[211]_{\gamma} \frac{1}{\sqrt{2}} [L[31]_{\alpha} SF[211]_{\alpha} + L[31]_{\beta} SF[211]_{\beta}] \right) \tag{E37}
\end{aligned}$$

$$\begin{cases} SF[211]_{\alpha} = \frac{1}{\sqrt{2}} [S[31]_{\alpha} F[31]_{\gamma} - S[31]_{\gamma} F[31]_{\alpha}] \\ SF[211]_{\beta} = \frac{1}{\sqrt{2}} [S[31]_{\beta} F[31]_{\gamma} - S[31]_{\gamma} F[31]_{\beta}] \\ SF[211]_{\gamma} = \frac{1}{\sqrt{2}} [S[31]_{\alpha} F[31]_{\beta} - S[31]_{\beta} F[31]_{\alpha}] \end{cases}$$

$$\begin{aligned}
\varphi_{S[31]F[22]}^{L[31]SF[211]b} \left[\frac{1}{2} \frac{1}{2}, \frac{1}{2} \frac{1}{2} \right] &= \frac{1}{\sqrt{3}} \left(C[211]_{\beta} \frac{1}{\sqrt{2}} [L[31]_{\gamma} SF[211]_{\alpha} + L[31]_{\beta} SF[211]_{\gamma}] \right. \\
&\quad - C[211]_{\alpha} \frac{1}{\sqrt{2}} [L[31]_{\gamma} SF[211]_{\beta} - L[31]_{\alpha} SF[211]_{\gamma}] \\
&\quad \left. - C[211]_{\gamma} \frac{1}{\sqrt{2}} [L[31]_{\alpha} SF[211]_{\alpha} + L[31]_{\beta} SF[211]_{\beta}] \right) \tag{E38}
\end{aligned}$$

$$\begin{cases} SF[211]_{\alpha} = \frac{1}{2} [S[31]_{\alpha} F[22]_{\beta} + S[31]_{\beta} F[22]_{\alpha} + \sqrt{2} S[31]_{\gamma} F[22]_{\alpha}] \\ SF[211]_{\beta} = \frac{1}{2} [S[31]_{\alpha} F[22]_{\alpha} - S[31]_{\beta} F[22]_{\beta} + \sqrt{2} S[31]_{\gamma} F[22]_{\beta}] \\ SF[211]_{\gamma} = \frac{1}{\sqrt{2}} [S[31]_{\alpha} F[22]_{\beta} - S[31]_{\beta} F[22]_{\alpha}] \end{cases}$$

$$\begin{aligned}
\varphi_{S[22]F[31]}^{L[31]SF[211]c} \left[\frac{1}{2}, \frac{1}{2}, \frac{1}{2} \right] &= \frac{1}{\sqrt{3}} \left(C[211]_{\beta} \frac{1}{\sqrt{2}} [L[31]_{\gamma} SF[211]_{\alpha} + L[31]_{\beta} SF[211]_{\gamma}] \right. \\
&\quad - C[211]_{\alpha} \frac{1}{\sqrt{2}} [L[31]_{\gamma} SF[211]_{\beta} - L[31]_{\alpha} SF[211]_{\gamma}] \\
&\quad \left. - C[211]_{\gamma} \frac{1}{\sqrt{2}} [L[31]_{\alpha} SF[211]_{\alpha} + L[31]_{\beta} SF[211]_{\beta}] \right) \quad (E39) \\
\begin{cases} SF[211]_{\alpha} = \frac{1}{2} [F[31]_{\alpha} S[22]_{\beta} + F[31]_{\beta} S[22]_{\alpha} + \sqrt{2} F[31]_{\gamma} S[22]_{\alpha}] \\ SF[211]_{\beta} = \frac{1}{2} [F[31]_{\alpha} S[22]_{\alpha} - F[31]_{\beta} S[22]_{\beta} + \sqrt{2} F[31]_{\gamma} S[22]_{\beta}] \\ SF[211]_{\gamma} = \frac{1}{\sqrt{2}} [F[31]_{\alpha} S[22]_{\beta} - F[31]_{\beta} S[22]_{\alpha}] \end{cases}
\end{aligned}$$

Appendix F: Chiral relation between T_{σ} and T_{π} in the Foldy-Wouthuysen reduction

The operators in (57) and (58) originate from the relativistic Yukawa couplings

$$\mathcal{L}_{\text{int}} = g_{\sigma} \bar{q} q \sigma + i g_{\pi} \bar{q} \gamma_5 \tau^a q \pi^a. \quad (F1)$$

Under an infinitesimal axial (chiral) transformation

$$q \rightarrow \left(1 + \frac{i}{2} \epsilon^a \tau^a \gamma_5 \right) q, \quad \bar{q} \rightarrow \bar{q} \left(1 + \frac{i}{2} \epsilon^a \tau^a \gamma_5 \right), \quad (F2)$$

the bilinears mix as

$$\delta(\bar{q} q) = i \epsilon^a \bar{q} \gamma_5 \tau^a q, \quad \delta(\bar{q} i \gamma_5 \tau^a q) = -i \epsilon^a \bar{q} q, \quad (F3)$$

so the scalar and pseudoscalar vertices are chiral partners at the relativistic level.

To connect this to (57) and (58), we perform a Foldy-Wouthuysen (FW) reduction of the Dirac Hamiltonian

$$H = \boldsymbol{\alpha} \cdot \mathbf{p} + \beta m + \beta g_{\sigma} \sigma + i \beta g_{\pi} \gamma_5 \tau^a \pi^a. \quad (F4)$$

Decomposing $H = \beta m + \mathcal{E} + \mathcal{O}$ into even and odd parts,

$$\mathcal{E} = \beta g_{\sigma} \sigma, \quad \mathcal{O} = \boldsymbol{\alpha} \cdot \mathbf{p} + i \beta g_{\pi} \gamma_5 \tau^a \pi^a, \quad (F5)$$

The σ -interaction is even ($[\beta, \mathcal{E}] = 0$), whereas the π -interaction is odd ($\{\beta, \mathcal{O}\} = 0$). This grading determines the order at which spin-dependent operators appear in the $1/m$ expansion. Keeping terms linear in the meson fields and expanding to the first nontrivial spin-dependent order, the FW Hamiltonian yields:

a. Pion vertex (odd operator). From the interference term in \mathcal{O}^2 one obtains, for positive-energy components,

$$H_{\text{FW}}^{(\pi)} = -\frac{i g_{\pi}}{2m} \boldsymbol{\sigma} \cdot \nabla (\tau^a \pi^a) + \mathcal{O}\left(\frac{1}{m^2}\right). \quad (F6)$$

In momentum space (\mathbf{q} the momentum transfer),

$$V_{\pi} = -\frac{g_{\pi}}{2m} \boldsymbol{\sigma} \cdot \mathbf{q} \tau^a. \quad (F7)$$

Thus the pseudoscalar coupling produces the leading nonrelativistic spin-momentum structure $\mathbf{S} \cdot \mathbf{q} \tau^a$.

b. Sigma vertex (even operator). The spin-dependent contribution arises from the double commutator term

$$-\frac{1}{8m^2} [\boldsymbol{\alpha} \cdot \mathbf{p}, [\boldsymbol{\alpha} \cdot \mathbf{p}, \beta g_{\sigma} \sigma]], \quad (F8)$$

which yields

$$V_{\sigma} = -\frac{i g_{\sigma}}{2m^2} \boldsymbol{\sigma} \cdot (\mathbf{p}' \times \mathbf{p}) + \mathcal{O}\left(\frac{1}{m^3}\right). \quad (F9)$$

Hence the scalar coupling generates the non-relativistic spin-orbit structure $\mathbf{S} \cdot (\mathbf{p}' \times \mathbf{p})$.

c. Light-front kinematics. Defining $K = (\mathbf{p}' + \mathbf{p})/2$ and $\mathbf{q} = \mathbf{p}' - \mathbf{p}$, one has $\mathbf{p}' \times \mathbf{p} = -K \times \mathbf{q}$. In the light-front $K \simeq K_z \hat{\mathbf{z}}$, so

$$\boldsymbol{\sigma} \cdot (\mathbf{p}' \times \mathbf{p}) \rightarrow \boldsymbol{\sigma} \cdot (\hat{\mathbf{z}} \times \mathbf{q}). \quad (F10)$$

Projecting the momentum transfer onto the intrinsic Jacobi coordinate, $\mathbf{q} \rightarrow \mathbf{p}_{\delta}$, the transition operators become

$$T_{\sigma} \propto \mathbf{S} \cdot (\hat{\mathbf{z}} \times \mathbf{p}_{\delta}), \quad T_{\pi} \propto (\mathbf{S} \cdot \mathbf{p}_{\delta}) \tau^a, \quad (F11)$$

which are (57) and (58)

Chiral symmetry relates the scalar and pseudoscalar quark bilinears at the relativistic level. After FW reduction, the even/odd grading of the Dirac operators causes the chiral partners to appear at different orders in the $1/m$ expansion. The pseudoscalar coupling produces the leading spin-momentum operator, while the scalar coupling produces the spin-orbit operator. These reduce in the light-front intrinsic basis precisely to T_{σ} and T_{π} as given by (57) and (58)

-
- [1] S. J. Brodsky, H.-C. Pauli, and S. S. Pinsky, *Phys. Rept.* **301**, 299 (1998), [arXiv:hep-ph/9705477](#).
- [2] X. Ji, *Phys. Rev. Lett.* **110**, 262002 (2013), [arXiv:1305.1539 \[hep-ph\]](#).
- [3] N. Isgur and G. Karl, *Phys. Rev. D* **18**, 4187 (1978).
- [4] L. Y. Glozman and D. O. Riska, *Phys. Rept.* **268**, 263 (1996), [arXiv:hep-ph/9505422](#).
- [5] D. Diakonov, V. Petrov, and M. Polyakov, *Z. Phys. A* **359**, 305 (1997), [arXiv:hep-ph/9703373](#).
- [6] R. F. Dashen, E. Jenkins, and A. V. Manohar, *Phys. Rev. D* **49**, 4713 (1994), [arXiv:hep-ph/9310379](#).
- [7] C.-R. An et al., *Phys. Rev. C* **85**, 055203 (2012), [arXiv:1203.5336 \[nucl-th\]](#).
- [8] C. Alexandrou et al., *Phys. Rev. D* **102**, 054517 (2020), [2006.00964](#).
- [9] N. Miesch, E. Shuryak, and I. Zahed, (2025), [arXiv:2510.23404 \[hep-ph\]](#).
- [10] E. Shuryak and I. Zahed, (2026), [arXiv:2601.15085 \[hep-ph\]](#).
- [11] D. Johnson, I. Polyakov, T. Skwarnicki, and M. Wang, *Ann. Rev. Nucl. Part. Sci.* **74**, 583 (2024), [arXiv:2403.04051 \[hep-ex\]](#).
- [12] L. Micu, *Nucl. Phys. B* **10**, 521 (1969).
- [13] A. Le Yaouanc, L. Oliver, O. Pene, and J. C. Raynal, *Phys. Rev. D* **8**, 2223 (1973).
- [14] A. De Rujula, H. Georgi, and S. L. Glashow, *Phys. Rev. D* **12**, 147 (1975).
- [15] A. Kock, Y. Liu, and I. Zahed, *Phys. Rev. D* **102**, 014039 (2020), [arXiv:2004.01595 \[hep-ph\]](#).
- [16] F. He, E. Shuryak, W. Wu, and I. Zahed, *Phys. Rev. D* **113**, 054015 (2026), [arXiv:2510.02076 \[hep-ph\]](#).
- [17] S. Capstick and W. Roberts, *Phys. Rev. D* **49**, 4570 (1994), [arXiv:nucl-th/9310030](#).